Air Quality, Atmosphere & Health (2026) 19:42
https://doi.org/10.1007/s11869-026-01897-7

Aerosol pollution across the Indo-Gangetic plain and the Himalayas: Seasonal patterns and implications for air quality and climate

S. Ramachandran[1,2] · Maheswar Rupakheti[2]

Received: 30 July 2025 / Accepted: 4 December 2025

Abstract
This study utilizes new, high-quality ground-based observations to investigate seasonal variations in key aerosol optical and physical properties across entire Indo-Gangetic Plain (IGP), Himalayan foothills, and central Himalayas including southern Tibetan Plateau, for the first time. Seasonal average aerosol optical depth (AOD) is ≥0.3 across most of the region, indicating heavy pollution almost throughout the year, except at high altitude locations where AOD is 2–3 times lower. Pre-monsoon AOD levels are elevated due to additional emissions from seasonal sources such as agro-residue burning and forest-fires, and continental aerosols advected from polluted regions. Monsoon AODs are lower because rains suppress emissions from forest fires and garbage burning, significant seasonal sources such as brick production are almost absent as well as regional transport of emissions. Fine-mode aerosols contribute > 80% to AOD in post-monsoon and winter at almost all sites. Clean continental and clean marine aerosols dominate Himalayas, while urban-industrial and biomass burning aerosols are prevalent in Himalayan foothills and IGP, except in Karachi and Lahore where mixed aerosols are present in significant quantity. Aerosol volume size distributions are bimodal in all seasons, with modal radius at 0.1–0.3 μm (fine mode) and at 2–5 μm (coarse mode). A comparison revealed commonality of aerosols between Himalayas, Minsk (Belarus) and Dushanbe (Central Asia), at the same time demonstrating intra-regional variability of dominant aerosol types unique to Himalayas and IGP, providing valuable constraints for high-resolution chemistry-transport modelling, inputs to improve satellite retrievals, and deepen understanding of aerosol impacts on climate and ecosystems in this region.

Keywords Aerosol optical and physical properties · Fine mode fraction · Aerosol type · Regional analysis · IGP and Himalayas · Air quality and climate

Introduction

Aerosol pollution and air quality are global issues, and linked to climate as the amount of the pollutants present at the surface and in the column govern the physical and optical characteristics of aerosols which in turn determine their radiative forcing. The radiative forcing due to aerosols is negative (cooling) and masks the global warming (positive) due to greenhouse gases (Forster et al. 2021). Aerosols continue to contribute the largest uncertainty in the present climate as well as in future climate projections because of the lack of knowledge and uncertainties on the spatial and seasonal variations in a variety of aerosol characteristics, such as aerosol optical depth and size distribution (Forster et al. 2021). The uncertainty is larger over regions where aerosols exist in higher amounts, such as Asia, a global aerosol hotspot. Two other major aspects that contribute to the uncertainty in aerosol radiative forcing pertain to the lack of high-quality aerosol observations over a terrain with complex topography and the challenges associated in resolving them in models as a function of space and height, when aerosols are abundant and exhibit elevation-dependent features. The Indo-Gangetic Plain (IGP) and the Himalayas is one such region. The IGP, one of the largest river basins in the world, is a densely populated and heavily polluted region in the world. The Himalayas and its foothills, situated between the IGP (an aerosol source region) and the relatively pristine

✉ S. Ramachandran
ram@prl.res.in

[1] Physical Research Laboratory, Ahmedabad, India

[2] Research Institute for Sustainability - Helmholtz Centre Potsdam, Potsdam, Germany

Published online: 23 February 2026

Himalayan-Tibetan mountain regions, provides a unique environment, to examine the transport and transformation of aerosols on a seasonal scale. The sources of air pollution over the IGP and the Himalayan region are both natural (dust and sea salt), and human made (fossil fuel combustion, and biomass burning of fire-wood, forest fires).

The optical and physical characteristics of aerosols over the IGP have been investigated extensively using the Aerosol Robotic Network (AERONET) data, and satellite data (e.g., Moderate Resolution Imaging Spectroradiometer (MODIS) and Multiangle Imaging Spectroradiometer (MISR). However, most of the studies based on AERONET measured columnar aerosol properties were conducted over one or two locations (Singh et al. 2004; Eck et al. 2010; Giles et al. 2012; Kedia et al. 2014; Ramachandran and Rupakheti 2021), or only for a specific season (e.g., Giles et al. 2011). The spatial variations in aerosol characteristics over this region are discussed using remote sensing (MODIS and MISR) data (Prasad and Singh 2007; Dey and Di Girolamo 2011). Their results have clearly indicated that the features in aerosol characteristics (content, composition and type) exhibit significant spatial and seasonal differences within a spatial distance of about 500 km in the IGP (Dey and Di Girolamo 2011; Kedia et al. 2014), suggesting therefore, that generalization of aerosol features in the hotspot region could be erroneous. Further, aerosol properties obtained over the IGP and the Himalayas (including a couple of sites in the Himalayan foothills such as Pokhara, Hetauda, Kathmandu in Nepal) were analyzed in a few studies (Kedia et al. 2014; Gautam et al. 2011; Raatikainen et al. 2014; Cho et al. 2017). Almost all these investigations were corresponding to a particular season/year, based on a limited set of columnar aerosol properties (AOD), and/or only surface data (Gustafsson et al. 2009; Raatikainen et al. 2014; Cho et al. 2017). However, it still remains a challenge as the heavily polluted IGP, as well as the Himalayas, located in the downwind region that receives the pollution outflow, are inadequately sampled (Lawrence and Lelieveld 2010; Gustafsson and Ramanathan 2016).

The simulation of aerosol characteristics in climate models remains a significant challenge, particularly in high-altitude locations such as the Himalayan-Tibetan Plateau region. The region's complex terrain, coupled with intricate vertical and horizontal transport processes (e.g., convection, large regional circulations, and local mountain-valley circulation), contributes to this complexity (Forster et al. 2021; Myhre et al. 2013). Evidence regarding the climate change over the Himalayas is still inconclusive and estimates suffer from high uncertainly due to limited observational data (e.g., Krishnan et al. 2019; Forster et al. 2021). This is particularly true for the magnitudes and sign of regional aerosol distribution, their physical and chemical characteristics in both source regions, and downwind regions like the Himalayan mountain regions, resultant regional aerosol radiative forcing, notably that of the anthropogenic aerosols, which remain uncertain due to lack of regional scale observational characterization of aerosol properties and their seasonal variability (e.g., Krishnan et al. 2019; Forster et al. 2021). AERONET, with its global coverage, uniform calibration, stringent quality control, and relatively higher accuracy has become a critical benchmark (dataset) for assessing, validating, refining aerosol model simulations and satellite retrievals (Bond et al. 2013; Andrews et al. 2017). However, challenges persist. For example, assimilating AERONET observations into two-dimensional variational system can increase the analysis errors in regions with high AOD gradients (Rubin et al. 2017), such as the IGP, where aerosol prediction remains particularly difficult. These challenges (assimilation and simulation) are higher, during winter when aerosol loading and AODs are high), and during periods of increased dust abundance in some seasons, which exhibits strong gradients, as seen over the IGP, that results in only moderate correlations between observations and model outputs (Ramachandran et al. 2015; Rubin et al. 2017). While constraints introduced on AOD led to strong correlation between Modern-Era Retrospective Analysis for Research and Applications-2 (MERRA-2) model outputs and AERONET observations, significant discrepancies remain (e.g., MERRA-2 was less well correlated with AERONET) especially for dust AOD (Che et al. 2022). Furthermore, large differences between MODIS Deep Blue and MERRA-2 AOD were observed when AOD exceeded 0.3 (Che et al. 2022). Results from Coupled Model Intercomparison Project Phase 6 (CMIP6) model simulations and their ensemble mean revealed large inter-model differences in model estimates, and discrepancies with observed AOD magnitudes and trends over Asia, with high AODs across the IGP - a profound feature of aerosol loading in the region - missing in most model simulations (Ramachandran et al. 2022). Given that accurate past and current estimates and projections of radiative and climate impacts of aerosols depend on precise simulation of aerosol properties, this study provides observational constraints and underscores the pressing needs for current climate models, including those used in IPCC assessments, to improve their representation of magnitudes and trends of various aerosol properties.

This study comprehensively examines the seasonal variations in key columnar aerosol optical properties (e.g., content) and physical properties (e.g., size), which are crucial for understanding climate change, air quality, and other environmental changes observed over a large region. Thus, the analysis focuses on a large and diverse region, encompassing the entire IGP, the central Himalayan foothills, and

mountainous areas extending to the southern Tibetan Plateau. In this context, the primary motivation (objective) is to investigate the seasonal variations in physical and optical characteristics of aerosols across this region (Fig. 1) with whole-year data available at all AERONET sites considered in the study. The results are derived from a detailed analysis of aerosol characteristics that are constrained (considering seasonal variations in upper and lower bounds of aerosol properties) by high-quality ground-based observations. These results are essential for improving global circulation/regional climate/chemistry transport models and for enhancing satellite retrievals to better validate, simulate, and predict climate change in this highly uncertain and sensitive region. The study's novelty lies in the seasonal analysis of data from all 13 sites which is observational data-intensive approach (Table 1), and statistical robustness. It leverages new, high-quality ground-based column observations of multiple aerosol parameters from thirteen distinct locations (including recently established AERONET sites in the Himalayan region), covering a large spatial domain within a climate-sensitive hotspot of global significance. This extensive dataset enables the identification of seasonal-scale variations with unprecedented accuracy. By presenting the observational evidences and constraints, the study provides critical insights that have significant implications for advancing aerosol science, refining climate models, and enhancing our understanding of regional and global climate change, particularly quantification of impacts of aerosols, a major current and future driver of regional climate change in South Asia.

The study region and its importance

The Indo-Gangetic plain (IGP) (Fig. 1), covers parts of Pakistan, India, Bangladesh and Nepal. Studies conducted during the last decades in this region as mentioned above, provided a basic and a broad understanding on the variations in aerosol characteristics and radiative forcing (Textor et al. 2006; Lawrence and Lelieveld 2010; Ramachandran et al. 2015; Ramachandran and Rupakheti 2021). MODIS Terra version 6.1 monthly level-3 aerosol optical depth (AOD) data at 0.55 µm retrieved using the Combined Dark Target and Deep Blue algorithms for land and ocean, and the AOD retrieved using the Dark Target algorithm for land are used to derive seasonal averages (Fig. 2). The expected

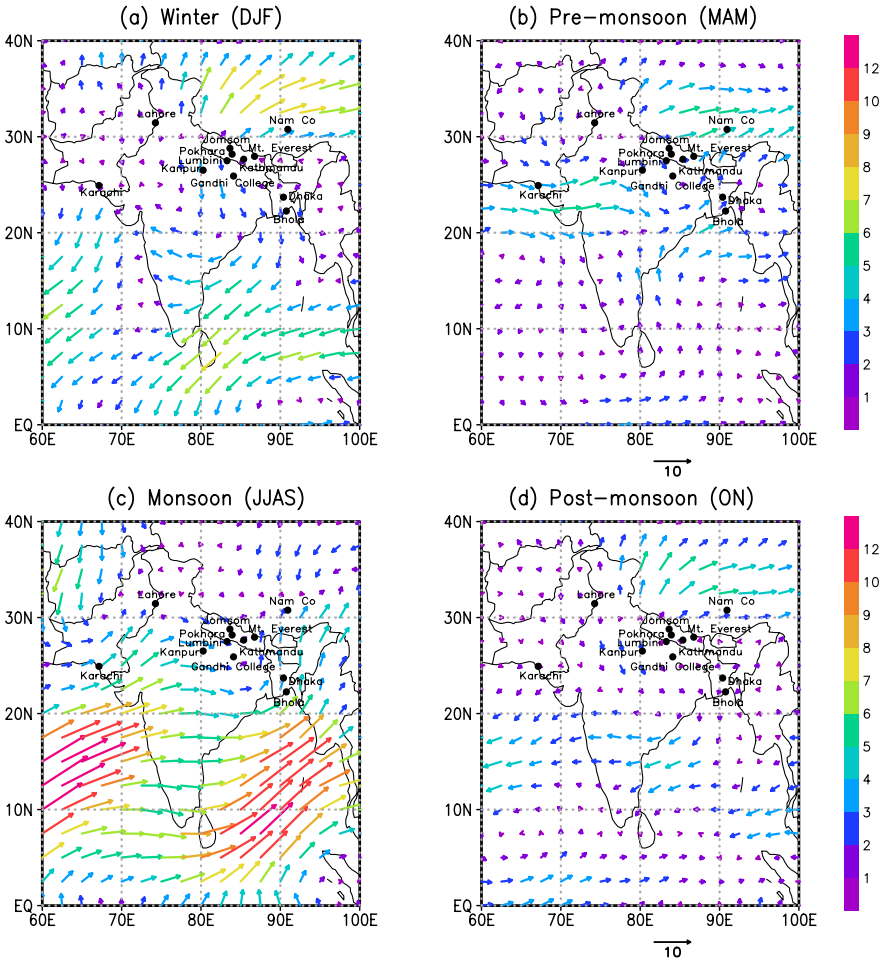

Fig. 1 Seasonal average synoptic winds (in ms^{-1}) at 850 hPa over the Indo-Gangetic Plain and the foothills of the Himalayas during (**a**) winter (DJF), (**b**) pre-monsoon (MAM), (**c**) monsoon (JJAS) and (**d**) post-monsoon (ON) for 2012. Wind data are downloaded from http://www.esrl.noaa.gov/psd/. Study locations in the IGP and the Himalayas are marked in the figure

Table 1 Study location details (latitude, longitude, and elevation in meters (m) above mean sea level), and data available at each location in different seasons. Number of days on which quality-controlled level 2 AERONET data on the above mentioned aerosol properties were available and utilized in each season along with their total

Location	DJF	MAM	JJAS	ON	Total
Himalayas:					
1. Jomsom, Nepal (28.8°N, 83.7°E, 2825 m)	62	84	93	57	296
2. Ev-K2-CNR/Mt. Everest, Nepal (27.9°N, 86.8°E, 5079 m)	70	79	45	32	226
3. Nam Co, Tibet, China (30.8°N, 90.9°E, 4746 m)	30	73	50	13	166
Himalayan foothills:					
4. Pokhara, Nepal (28.2°N, 83.9°E, 800 m)	83	84	70	57	294
5. Kathmandu, Nepal (27.7°N, 85.4°E, 1297 m)	81	76	59	41	267
Western IGP:					
6. Karachi, Pakistan (24,9°N, 67.1°E, 49 m)	81	80	49	19	229
7. Lahore, Pakistan (31.4°N, 74.3°E, 209 m)	58	82	107	56	303
8. New Delhi, India (28.6°N, 77.2°E, 240 m)	31	46	48	14	139
Central IGP:					
9. Lumbini, Nepal (27.5°N, 83.3°E, 110 m)	45	78	48	48	224
10. Kanpur, India (26.5°N, 80.2°E, 123 m)	54	72	63	29	218
11. Gandhi College, India (25.9°N, 84.1°E, 60 m)	64	82	78	58	282
Eastern IGP:					
12. Dhaka, Bangladesh (23.7°N, 90.4°E, 34 m)	76	70	52	54	252
13. Bhola, Bangladesh (22.2°N, 90.8°E, 7 m)	81	80	37	48	246

error in MODIS AODs is ±(0.05 ± 0.15xAOD) over land (Levy et al. 2013). The MODIS AOD maps are drawn to portray the spatial distribution and for representativeness of AODs over the study region (Fig. 2). It is clear from the figure that the IGP is heavily polluted as AODs often exceed 0.3 during the year (Fig. 2) highlighting the importance of the region. We extend the focus of these observations, providing a heretofore not available space-time scenario of aerosols over the IGP and the Himalayas using new and high-quality ground-based columnar observations. The columnar content of aerosols, and size distribution parameters measured with ground-based CIMEL Sun/sky radiometers at the thirteen AERONET (Holben et al. 2001) sites in the region (Table 1) are analyzed in the study. Though satellites can provide global coverage on aerosols, the accuracy and resolution are lower (Schutgens et al., 2017). During the monsoon season, it is cloudy and overcast over the IGP, due to which satellite retrievals could be affected, as there exists no perfect cloud mask (Levy et al. 2013). Further, as a global uncertainty of ± 0.03 could be quite high to constrain aerosol forcing, AOD observations from MODIS may be used as support in studies that combine models, in situ observations and other satellite data sets for reducing the uncertainty (e.g., Levy et al. 2013 and references therein). MODIS and MISR were found to underestimate/overestimate when compared to the ground-based AERONET AODs (Ramachandran and Kedia 2013). For example, 3-year (2006–2008) annual average MODIS AODs over the IGP exhibit biases, being overestimated by 0.06 (~ 10%) in Kanpur (AOD = 0.63) and underestimated by 0.07 (~ 10%) in Gandhi College (AOD = 0.68) compared to AODs from AERONET measurements (Ramachandran and Kedia 2013). Similarly, for the same time period MISR underestimated AOD by 0.02–0.17 over Karachi and Kanpur, while overestimating AOD by 0.20 in Gandhi College relative to AERONET. In addition, remote sensing observations can only retrieve fewer aerosol characteristics, for example AOD, as compared to ground-based measurements which remains a limitation. Aerosol extinction available from Cloud-Aerosol Lidar and Infrared Pathfinder Satellite Observation (CALIPSO) at a 40-km horizontal resolution is uncertain by about 40% (http://wdc.clr.de/sensors/calipso). CALIPSO repeats its orbit every 16 days over the same location (i.e., about two over passes per month over a particular location), as a result its sampling frequency is lower. In contrast, ground-based columnar measurements available almost every day of the year are far more accurate, and are best suited to investigate the seasonal variations in aerosols. The AERONET sites are located in the IGP and the central Himalayan foothills, and Himalayan-Tibetan Plateau region (Fig. 1; Table 1). The environmental settings of these locations vary - Karachi, Lahore, New Delhi, Kanpur and Dhaka are urban, industrial and densely populated cities. Kanpur is located ~ 500 km downwind of the megacity New Delhi. Karachi is an urban/coastal location. Gandhi College is a rural location in the central IGP. Bhola is the largest island in southern Bangladesh in the Bay of Bengal. The five sites in Nepal are located at differing altitudes and have markedly varying environmental ambience in terms of geography and urbanization. Lumbini is a rural area. Kathmandu and Pokhara in Nepal are valleys in the Himalayan foothills and are the largest and second largest metropolitan regions, respectively. Jomsom is a hill station in the Himalayan mountain region and a commercial center located on the banks of Gandaki River. The AERONET Ev-K2-CNR (hereinafter referred to as Mt. Everest) is set up at the Nepal Climate Observatory at Pyramid (NCOP), a high-altitude scientific observatory located near the base camp of Mt. Everest in the Himalayas in Nepal. Nam Co is an alpine meadow in southern Tibetan Plateau. These locations are often downwind of the IGP (Figs. 1 and 3).

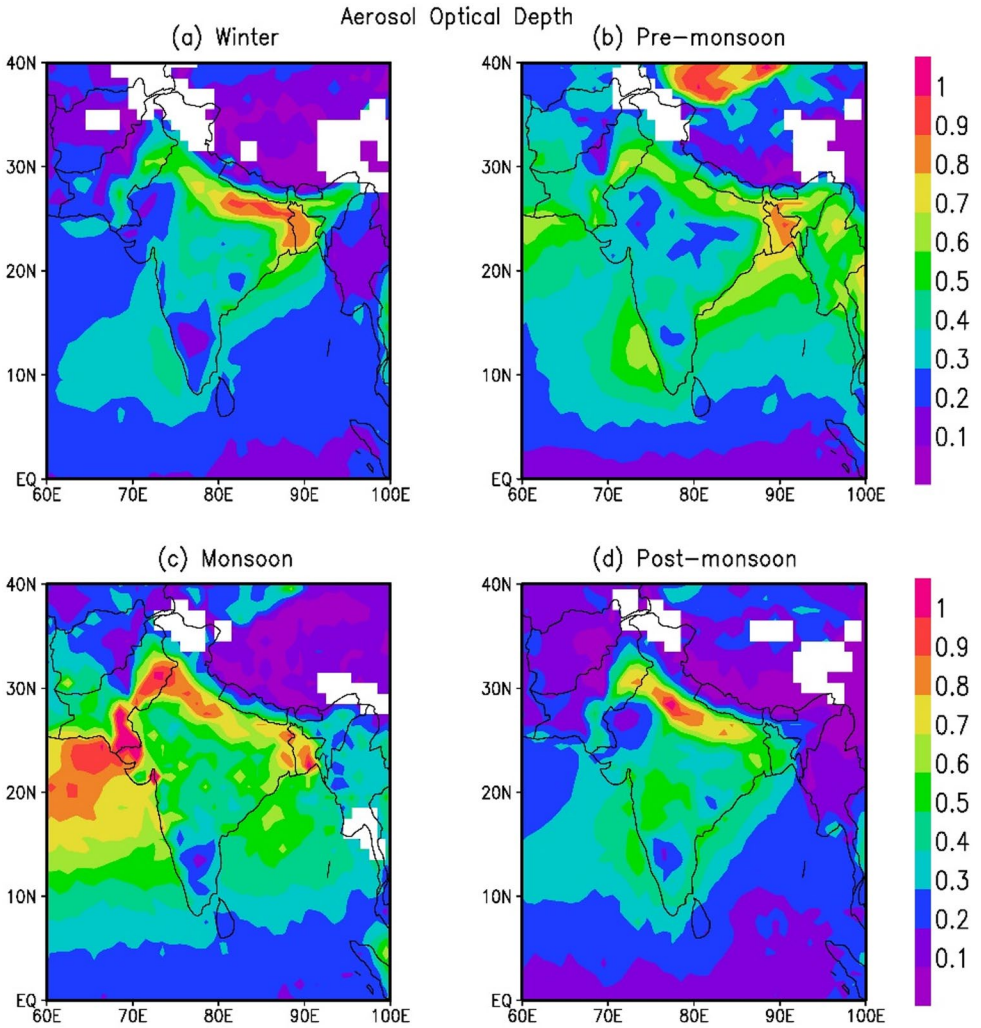

Fig. 2 Seasonal average MODIS Terra v6.1 AOD retrieved using the Combined Dark Target and Deep Blue algorithms for land and ocean, and the AOD retrieved using the Dark Target algorithm for land (0.55 μm) over the Indian subcontinent for (**a**) winter, (**b**) pre-monsoon, (**c**) monsoon and (**d**) post-monsoon of 2012, downloaded from https://giovanni.gsfc.nasa.gov/giovanni/

The physical, optical and chemical characteristics of aerosols over a particular location/region depend on emission sources, meteorology (winds, rainfall, relative humidity and atmospheric boundary layer), and atmospheric dynamics including long-range transport on a seasonal scale (Kedia et al. 2014). Aerosols originate from diverse sources such as oceans, deserts, industries, vehicles, and biomass burning. They are produced through both primary and secondary processes, including gas-to-particle conversion, winds, chemical reactions, primary emissions, and mechanical generation. These processes result in various aerosol types, including sulfate, nitrate, black carbon, organic carbon, organic matter, and dust. In aerosol size distribution, the number of aerosols in fine-mode (≤1 μm in radius) is orders of magnitude higher than that of coarse-mode particles (≥1 μm in radius). Fine-mode aerosols contribute over 90% to aerosol extinction in the mid-visible wavelengths over continental and urban regions, while in the marine environments, their contribution drops to around 60% (Ramachandran 2018). In contrast, coarse-mode aerosols, such as desert dust, dominate extinction (>60%) in arid regions (Ramachandran 2018). The modal radius of aerosols varies by type: water soluble particles, sulfate, black carbon, organic carbon, insoluble (mostly soil particles with a certain amount of organic material), mineral dust, and sea salt in fine-mode (nucleation and accumulation modes) typically have radii ≤0.50 μm, whereas coarse-mode mineral dust and sea salt have radii >1.5 μm (Hess et al. 1998).

Hygroscopic aerosols, such as water soluble particles, sulfate, and sea salt swell with increasing relative humidity (RH) and shrink when RH decreases. This process alters their size, composition, optical and radiative characteristics. Among the hygroscopic aerosols, when RH is increased from 0% to 95%, water-soluble aerosols grow from a modal radius of 0.02 μm to 0.04 μm, sea salt (accumulation mode) increases from 0.21 μm to 0.61 μm, the sea salt (coarsemode) grows from 1.75 μm to 5.11 μm, and sulfate aerosols increases from 0.07 μm to 0.16 μm (Hess et al. 1998). Despite these changes, fine-mode aerosols remain within the fine-size range, and

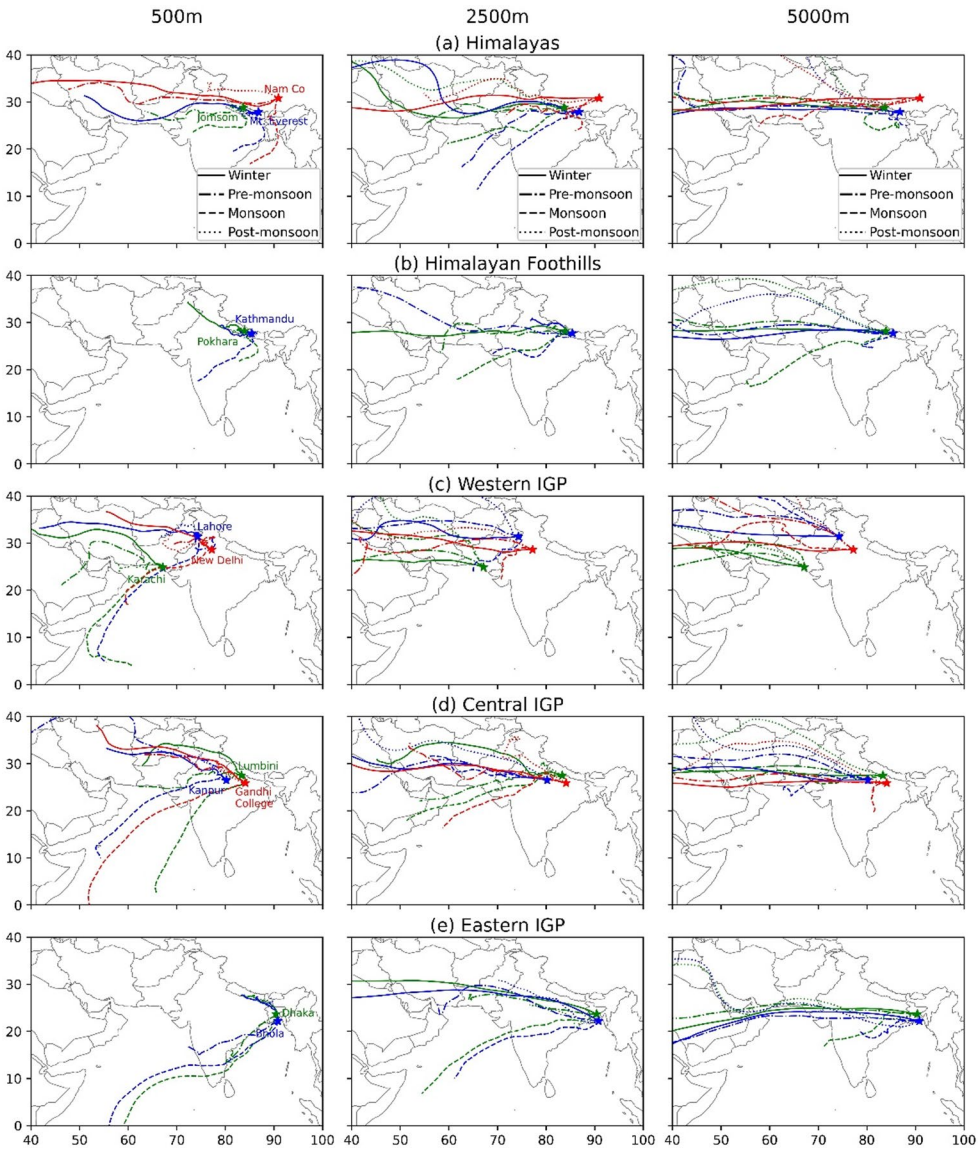

Fig. 3 Seasonal (winter, pre-monsoon, monsoon and post-monsoon) averages of 7-day air back trajectories at 500 m, 2500 m and 5000 m agl corresponding to 0600 UTC for the study locations in the (**a**) Himalayas, (**b**) Himalayan foothills, (**c**) Western Indo-Gangetic Plain (IGP), (**d**) Central IGP and (**e**) Eastern IGP for winter (DJF), pre-monsoon (MAM), monsoon (JJAS) and post-monsoon (ON) seasons of 2012. Stars represent the location; the location and the back trajectories at each elevation for different seasons are drawn with different labels in the same color

coarse-mode aerosols stay within the coarse range. While RH may significantly impact surface-level aerosol number or mass concentrations of a particular water-soluble aerosol species, its effect on AOD, which is a measure of total columnar extinction due to aerosols in the radius range of 0.01 to 10 µm, depends on the overall aerosol composition and the contribution of a particular aerosol species in the atmospheric column. The impact of RH on AOD varies with aerosol type (e.g., components, number densities) and environmental setting of the location/region. In desert-dominated regions, where non-hygroscopic dust is abundant, changes in RH have minimal impact on AOD. In marine regions, where hygroscopic aerosols dominate, RH has a much larger effect (AOD increases by >100% when RH increases from 0% to 95%) (Hess et al. 1998). This sensitivity is particularly relevant in South Asia, where aerosols from anthropogenic and natural sources coexist, exhibiting significant spatial and temporal variabilities depending on source type, season, and transport (Ramachandran et al. 2020).

The climate over this region is humid and subtropical with hot, humid summer and cold, dry winter. The South Asian monsoon influences all the study locations in this region (Table 1), where winds are southwesterly during the summer monsoon and northeasterly during the winter monsoon, respectively (Lawrence and Lelieveld 2010; Kedia et al. 2014; Ramachandran et al. 2015, 2022; Singh et al. 2019). The seasons in South Asia are classified as winter (DJF - Dec-Jan-Feb), pre-monsoon (MAM - Mar-Apr-May), monsoon (JJAS - Jun-Jul-Aug-Sep) and post-monsoon (ON - Oct-Nov). The prevalent meteorological conditions and atmospheric dynamics, including long-range transport significantly influence the temporal and seasonal characteristics of aerosols in a region (Kedia et al. 2014). The winds are calmer during winter over the

IGP and the Himalayas (Fig. 1a), northerly/northeasterly favoring accumulation of both local and regionally transported emissions which give rise to the annually recurrent regional scale atmospheric haze (Ramanathan et al. 2007; Lawrence and Lelieveld 2010; Ramachandran et al. 2022). The winds during pre-monsoon, and monsoon (or rainy season) which originate from the southwesterly direction are stronger than winter; these stronger winds transport dust from arid regions (during pre-monsoon and monsoon seasons), and sea salt from the maritime regions and dust from deserts during monsoon (Fig. 1). In post-monsoon the winds undergo a directional transition and shift from southwest to northeast, and are comparatively quite calmer (Fig. 1d) than the other three seasons (Fig. 1). In winter temperature and wind speed are lower over the IGP, and the atmosphere is dry because of low RH. During pre-monsoon temperature and wind speeds increase. RH becomes high in monsoon during which South Asia receives heavy and most of the rain of the year. Whereas in post-monsoon temperature, wind speeds and RH become lower (Ramachandran et al. 2015, 2020). The atmospheric boundary layer is shallow (< 500 m) during post-monsoon and winter over the IGP whereas it is deeper during pre-monsoon and monsoon (extending up to 4 km) (Singh et al. 2019; Ramachandran et al. 2020), which have implications to AOD, FMF and α variations discussed later.

To identify the source regions and the transport pathways of pollutants before they reach the measurement locations, airmass back trajectory analysis was performed (Fig. 3). Using the Hybrid Single-Particle Lagrangian Integrated Trajectory (HYSPLIT) model (Draxler and Hess 1998), 7-day back trajectories are calculated at 0600 Coordinated Universal Time (UTC) for all the study locations (Table 1; Fig. 3). These trajectories are calculated at three altitudes (heights above the ground): 500 m represents the mixed layer height, 2500 m captures aerosols lifted above the boundary layer by convection and transported over long distances, and 5000 m corresponds to the free troposphere. This multi-level analysis helps explain the variability in aerosol properties within the atmospheric column. Overall, the transport pathways and the source regions across all study sites show similarity but exhibit distinct seasonal variations (Fig. 3). During winter, pre- and post-monsoon, the air masses predominantly originate from and traverse the west at all three heights. During monsoon, winds primarily originate over the Arabian Sea, changing in direction from west to southwest, and pass over the continent before reaching the measurement locations (Fig. 3). The analysis of potential aerosol source regions, transport pathways, and associated meteorological parameters (winds, atmospheric boundary layer) (Fig. 1) provides valuable insights for interpreting seasonal variations in columnar aerosol characteristics.

Data and analysis

The level 2, version 3 cloud screened and quality assured daily data, updated from the previous version and includes improved cloud screening and quality control methods, cirrus cloud detection and removal (Sinyuk et al. 2020), on aerosol optical depth (AOD), fine mode fraction (FMF), Ångström exponent (α), aerosol volume size distribution, volume mixing ratio and effective radii were obtained from the following AERONET sites for a period of a year: Jomsom (Jan-Dec 2012), Mt. Everest (Nov 2011-Oct 2012), Nam Co (Oct 2012-Sep 2013), Pokhara (Jan-Dec 2012), Bode, Kathmandu (Jan-Dec, 2013), Karachi and Lahore (Jan-Dec 2012), New Delhi (Jan-Dec 2009), Lumbini (Jan-Aug 2013 and Sep-Dec 2017), Kanpur and Gandhi College (Jan-Dec 2012), and Dhaka (Jan-Dec 2014) and Bhola (Jan-Dec 2015) (Table 1). Since, the objective is to cover one annual cycle along with seasons over the study locations/region, data sets corresponding to the years 2013-15 were utilized (or for 2012 in case if data were not available for 2013–2015). The period covering 2012–2015 was chosen, since simultaneously collected data were available for almost all the months (covering all the four seasons mentioned above) in all the locations in this time period only (Table 1). Aerosol data for New Delhi throughout the year were available only for the year 2009, which are utilized in this study (Table 1) (Ramachandran and Rupakheti 2021). This method of analyzing the data available in the precedent year(s), and/or later year(s) with respect to the select year(s) is quite robust, and is not expected to influence significantly the consequent scientific outcomes as the data are from the same instrument with the same level of quality control, the seasonal variations in aerosols are more prominent than inter-annual variations in South Asia (Lawrence and Lelieveld 2010; Kedia et al. 2014; Ramachandran et al. 2015, 2022; Ansari and Ramachandran 2023), and changes in AODs were minimal due to the changes (increase/decrease) in anthropogenic activity and meteorology during a 5-year period (Ramachandran et al. 2015; Zhang et al. 2019). As the data over multiple sites for different years were unavailable simultaneously, statistical significance of interannual variations in aerosol properties could not be determined for each site. However, the inter-annual variability in aerosol properties (AOD, α, and FMF) during 2015–2019 over two sites in the IGP (Kanpur and Gandhi College) were found to be statistically insignificant as the p-value was > 0.05 at 95% confidence level (calculated using two-tailed Student's t-test) (Ansari and Ramachandran 2023).

AERONET measurements

The field of view of the Sun/sky radiometer instrument is 1.2°. The radiometer makes direct solar radiation

measurements approximately every 15 min under clear-sky conditions, which typically results in about 20 measurements every day. The aerosol products derived from direct solar measurements at four spectral channels (0.44, 0.50, 0.675, and 0.87 μm), and sky radiance measurements made at four spectral channels (0.44, 0.675, 0.87 and 1.02 μm) are utilized in the study. The aerosol properties retrieved from AERONET measurements have the highest accuracy in the solar zenith angle range of 50° and 80° (Dubovik et al. 2000), and only those data points in a day that are within this solar zenith angle range are utilized in the study. The uncertainty in AODs from the direct solar radiation measurements is less than ±0.01 for wavelengths > 0.44 μm (Holben et al. 2001). The error in AERONET derived FMF is ~10% (O'Neill et al. 2003). The spectral AODs follow a power law of the form $y = K\lambda^{-\alpha}$, where λ is the wavelength, y is AOD, and α is AE, respectively. AE (α) is derived using AODs measured at 0.44, 0.50, 0.675 and 0.87 μm by least squares fitting of AOD with respect to wavelength on a log-log plot. The errors in volume size distributions are not significant in the sub-micron and micron radius range (Dubovik et al. 2002). At the three high-altitude AERONET sites, Jomsom, and Mt. Everest (Nepal), and Nam Co on the Tibetan Plateau (China) (Table 1) AOD, FMF and Ångström exponent (α) derived from direct radiation measurements (Direct Sun Algorithm) only are available, whereas the inversion products (volume aerosol size distribution, volume mixing ratio and effective radii) retrieved from direct and diffuse radiation measurements (Solar almucantar scenario in Inversion Algorithm) are unavailable. The daily averages of these aerosol parameters at each location are used to calculate the seasonal averages (Table 1). The number of data points are reduced during the monsoon season over the study region due to clouds (and hence by cloud screening in the AERONET algorithms).

Results and discussion

Aerosol optical depth, fine mode fraction and Ångström exponent

Himalayas and foothills

At the outset, AODs in the entire year are ≥0.3 over all the locations except the high altitude locations (Fig. 4a), confirming that the entire region is heavily polluted. However, the seasonal variations in AODs differ across the region (Figs. 2 and 4). AODs over four sites in Nepal are at their highest in MAM (pre-monsoon), lowest in JJAS (monsoon) and in between during ON (post-monsoon), whereas Lumbini in Nepal has the highest AOD in post-monsoon followed by pre-monsoon, monsoon and DJF (winter) (Fig. 4a). AODs at the high altitude sites in the Himalayas (Jomsom, Mt. Everest and Nam Co) are lower than AODs at the sites in foothills and southern plain by a factor of 2 to 3 (Fig. 4a). Even in these high altitude locations pre-monsoon AOD is highest and the post-monsoon AODs are the lowest; during pre-monsoon Jomsom AOD is ~0.2 while AODs at Nam Co and Mt. Everest are about a half of that at Jomsom. It is clear that AODs decrease as altitude increases in general, or remains almost the same beyond 4000 m asl (for example, Nam Co and Mt. Everest). The FMF at all sites is higher in post-monsoon and winter than in pre-monsoon and monsoon. The FMF in the high altitude locations (Mt. Everest and Nam Co) is lower than that in Jomsom (Fig. 4b) and the other locations in Nepal i.e. Lumbini, Pokhara and Kathmandu (Fig. 4b). The FMF is >0.80 during ON (post-monsoon) and DJF (winter) over Lumbini, Pokhara and Kathmandu, which decreases in MAM (pre-monsoon) and JJAS (monsoon). The Ångström exponent (α) depends on aerosol size distribution; higher α values (>1) indicate the dominance of fine mode aerosols (produced from combustion sources (coal fired power plants), industrial and vehicular emissions and domestic biomass burning (fuel wood and dung cake)), while lower α (<1) occur due to the domination of coarse mode aerosols (dust and sea salt) in aerosol size distribution. Among the Himalayan sites, α is >1 over Jomsom throughout the year, while α at the other two sites is ca. 0.5–1.0 (Fig. 4c). The lower α values at these sites are consistent with their lower FMF (Fig. 4b), and decrease further as the elevation increases from Jomsom to Mt. Everest (except during post-monsoon when α over Nam Co is nearly equal to that of Mt. Everest); this suggests that once the altitude of the location is beyond 4000 m, and the aerosol content is quite less, the wavelength dependence of aerosols at the higher altitudes can be similar. The feature in α is ably corroborated by the FMF (Mt. Everest FMF is >Nam Co FMF (Fig. 4b)). The α is >1 throughout the year over Pokhara and Kathmandu, and seasonally less invariant (Fig. 4c). This is true in case of Lumbini as well, corroborating the consistent dominance of fine mode particles in the atmosphere up to the northern edge of IGP and the Himalayas.

The aerosol content during MAM is high over the Himalayan foothills (Singh et al. 2019) and further at higher altitudes in the Himalayas. The strong convection in this season aids air masses with pollution to get lifted to higher heights and advect northwards towards Himalayas (Kuhlmann and Quaas 2010; Singh et al. 2019). The advection of air masses during MAM is also aided by the strong updraft and a higher atmospheric boundary layer. The advected polluted air masses often get mixed with synoptic scale westerlies (Raatikainen et al. 2014; Putero et al. 2018; Singh

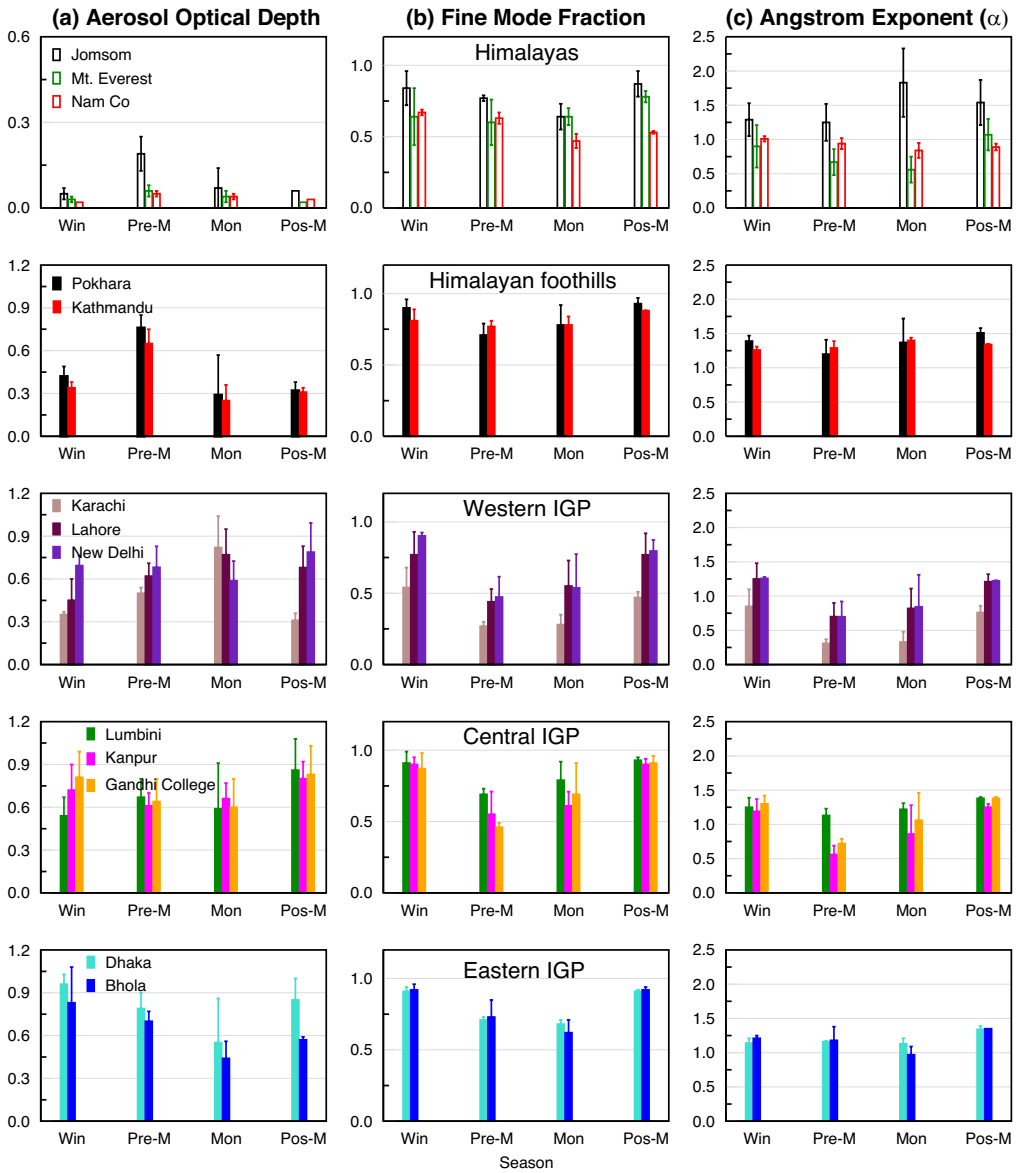

Fig. 4 Seasonal mean (**a**) aerosol optical depth (AOD) at 0.50 μm, (**b**) fine mode fraction (FMF) and (**c**) Angstrom exponent (α) over the study locations in Himalayas (Jomsom and Mt. Everest in Nepal, and Nam Co in Tibet, China), Himalayan foothills (Pokhara and Kathmandu in Nepal), western IGP (Karachi and Lahore in Pakistan, and New Delhi in India), central IGP (Lumbini in Nepal, and Kanpur and Gandhi College in India), and eastern IGP (Dhaka and Bhola in Bangladesh). Vertical bars denote the ±1σ standard deviation from the seasonal mean

et al. 2019), and give rise to high AOD during MAM. The emissions from forest fires and the subsequent transport get suppressed due to monsoon rains, and brick production in IGP and the valleys in the Himalayan foothills are less active in this season, due to which AODs are lower in JJAS at elevated locations. The low and similar values of AODs across three high-altitude sites in post-monsoon and winter (almost 3–9 times lower than the AODs over low lands) indicate that these sites remain mostly above the atmospheric boundary layer (ABL) over low lands in the south during the two seasons (Putero et al. 2018). The aerosols produced by fossil fuel and biomass burning emissions from urban conglomerates and transported to other regions are in fine mode, will be higher near the surface and their contribution to total AOD will decrease as the altitude increases, and in addition the coarse mode particles (dust) from the local dry and barren lands, and long-range transport are expected to be present at elevated locations resulting in lower FMF as seen here. FMF is higher at the foothills (Pokhara and Kathmandu, and also Lumbini) than other sites in pre-monsoon because these sites are affected by forest fires in the foothills and transport of agro-residue emissions from IGP, and less impacted by soil dust as foothills are mostly covered with forests. The high altitude sites also have wind-blown dust as

the lands around these sites are dry and barren. The seasonal variations in FMF are consistent with the findings of chemical composition analysis for PM_1 (particulate matter of diameter ≤ less than 1μm) and PM_{10} (particulate matter of diameter ≤ less than 10 μm) at the high-altitude Himalayan station, Nepal Climate Observatory – Pyramid (NCO-P), located at 5079 m asl near the Mt. Everest basecamp (Decesari et al. 2010). Dust concentrations were highest during pre-monsoon, followed by winter, monsoon, and post-monsoon. The lowest FMF at NCO-P in pre-monsoon (Fig. 4) confirms that increased coarse-mode dust during this season in this region reduces FMF. Aerosol species concentrations observed at NCO-P exhibited a consistent temporal pattern, peaking in pre-monsoon and dipping during monsoon, and gradually recovering in post-monsoon and winter (Decesari et al. 2010). Similar seasonal trends – high FMF in pre-monsoon and low during monsoon - were also observed at other Himalayan sites (e.g., Cho et al. 2017; Tripathee et al. 2017). These seasonal variations are attributed to seasonal changes in dry and moist convection and as well as wet scavenging processes (Decesari et al. 2010). The year-round mountain-valley wind circulation, active except during the monsoon, significantly affects the chemical composition of particulate matter in the high Himalayas, effectively transporting anthropogenic aerosols to altitudes exceeding 5000 m asl in the Asian region (Decesari et al. 2010). In contrast, mineral dust concentrations were predominantly influenced by multiple source regions in Central and Southwest Asia (Fig. 3), with limited contributions from valley breezes (Decesari et al. 2010). As we move from south to north (Lumbini, Pokhara, Kathmandu, Jomsom, Mt. Everest and Nam Co), the FMF decreases which is due to lesser influence of agricultural fires and forest fires, and higher influence of wind-blown dust (or may be ice particles too at high altitude locations).

Western, central and eastern IGP

Over Karachi (a sea port and dust influenced site) and Lahore (urban and dust influenced site) AODs are higher (>0.75) during monsoon than the other three seasons. AODs in these two locations keep increasing from winter to monsoon and then drop in post-monsoon (Fig. 4a). The higher RH during monsoon months (RH is 80% or higher across the study region (Ramachandran et al. 2015) aids the hygroscopic growth of aerosols (Sect. 2). The abundance of aerosols in coarse mode due to hygroscopic growth, and a deeper ABL which can accommodate more aerosols can increase AOD in monsoon as seen here. Interestingly, the AODs over all the three locations in India have a u-shaped structure (Fig. 4a) with AODs decreasing gradually from winter to monsoon, and then peaking up during post-monsoon. The AODs over these sites during winter and post-monsoon are comparable (ca. >0.7). Among the study locations and in all the seasons, the winter season AOD in Dhaka is the highest with a value ~ 1 (Fig. 4a). AODs over two stations in eastern IGP in Bangladesh also exhibit a similar character as that of the Indian stations, however, the seasonal differences in AODs are significantly higher in Bangladesh (Fig. 4a). Over the IGP AODs exhibit a west (high) to east (low) gradient during winter, which reverses during monsoon when AODs decrease from west to east. A shallow ABL, lower RH and calm winds during winter aid in accumulation of aerosols which combined with increasing emissions produce the observed spatial pattern over the IGP (Lawrence and Lelieveld 2010; Ramachandran et al. 2015, 2022), whereas the magnitude of decrease and the gradient seen in AODs during monsoon depend on the progression and strength of the monsoon from west to east; the AODs are significantly lower as a result of this in Bhola and Dhaka when compared to the other locations in IGP. The highest AOD for most of the year is observed over Dhaka (>0.8), with a more pronounced reduction during the monsoon compared to other locations. Rainfall across the IGP exhibits considerable spatial variability, decreasing by a factor of 2 to 3 from the east to west. For instance, in 2012, rainfall in Lahore was 360 mm, 822 mm in Kanpur, and 1257 mm in Dhaka. Consequently, the greater summer monsoon rain over Dhaka leads to a more substantial reduction in aerosol content through wet removal than the other IGP locations to the west of Dhaka like Kanpur and Lahore.

The high FMF in winter and post-monsoon, and low FMF in pre-monsoon and monsoon over the IGP locations is accordant with the increase in the abundance of coarse mode particles (dust and sea salt) across the IGP during pre-monsoon and monsoon, respectively (Kedia et al. 2014; Ramachandran et al. 2015, 2020). The FMF is consistently higher during the whole year over all the locations in Nepal (Fig. 4b) when compared to the other locations in the IGP highlighting a regional-scale dominant presence of aerosols in fine mode from emissions of fossil fuel and biomass burning through local and regional sources throughout the year over Nepal (Rupakheti et al. 2019). Among IGP sites, the seasonal values of α vary between 0.3 and 1.5 (Fig. 4c) with a visible seasonal variation over all sites (except Dhaka and Bhola) – lower during pre-monsoon and monsoon, and higher during winter and post-monsoon. It is consistent with the seasonal variation in FMF (Fig. 4b). During ON (post-monsoon) and DJF (winter) FMF and α are higher which corroborate the dominant contribution of fine mode aerosols to AOD, whereas lower FMF and α during MAM (pre-monsoon) and JJAS (monsoon) affirm a significant increase in the abundance of aerosols in coarse mode (e.g., sea salt, dust) in the columnar aerosol distribution over all sites in the

study region. The α values confirm the features observed in FMF (Fig. 4b, c) and is consistent with the aerosol type and size that dominate IGP and the Himalayas during different seasons. This linkage highlights that though the FMF (indicator of the dominant aerosol size) and α (relative measure of fine vs. coarse mode aerosols in the columnar aerosol size distribution) are comparable among the sites, the AOD (measure of columnar content) features differ because of the differences in emission sources of aerosols, their sizes, and their transport across the IGP and the Himalayas.

Inter-annual, and seasonal variabilities in aerosols across Himalayas and IGP

During the study period, the inter-annual variability within the sites (Kanpur, Gandhi College, Karachi, Lahore, and Pokhara) where long term aerosol data from AERONET were available was quite less (Ramachandran and Rupakheti 2022). The AOD levels and the differences across the sites were similar (Ramachandran and Rupakheti 2022) to those observed here (Fig. 2), thereby ruling out any caveats, if any, on the results in terms of inter-annual variability within and across the sites. Further, the inter-annual variation in AOD over Kanpur and Gandhi College in the IGP was found to be less than 10%, and it was even lower for FMF (< 5%) (Ansari and Ramachandran 2023), whereas the intra-annual (i.e., seasonal) variation is higher and statistically significant over most parts of the Himalayas and the IGP (Table 2), clearly emphasizing that the intra-annual variation in aerosol optical characteristics is more profound than their inter-annual variations over most parts of the study region. This occurs due to the significant changes in the amount and type of aerosol emissions as a function of season within a year depending on mainly the emissions from natural and anthropogenic activities, followed by meteorological conditions (winds, RH, ABL height) which vary on seasonal scales more significantly. The seasonal variations in AOD are not statistically significant at a few locations (e.g., Delhi and Kanpur) and during some seasons (mostly between monsoon and post-monsoon over most locations) either due to high AODs (0.6–0.8 during the year, Fig. 2) and/or due to less seasonal variation (AOD in winter is 0.7, remains the same in pre-monsoon decreases to 0.6 in monsoon and goes up to 0.8 in post-monsoon). However, the seasonal variation in α over both these locations are statistically significant most of the year except for the post-monsoon to winter season (Table 2). This occurs because while the AOD corresponds to the wavelength of 0.50 μm, α represents the spectral dependence of AODs measured in the 0.44–0.87 μm wavelength range, the values of which significantly vary across time and locations depending on the dominance of fine and/or coarse mode aerosols. In Delhi and Kanpur, AOD is > 0.6 throughout the year (Fig. 4) with negligible seasonal variation in magnitude, confirming that both sites are highly polluted, however, α values exhibit significant seasonal variations suggesting that AOD at 0.50 μm can be same for different α values. The α values are higher in winter and post-monsoon, and lower in pre-monsoon and monsoon. The α values are close (~0.9)

Table 2 Statistical significance of changes in aerosol optical depth and Ångström exponent between two consecutive seasons (Winter (Win) – Pre-monsoon (Pre-M), Pre-M – monsoon (Mon), Mon – Post-monsoon (Post-M), Post-M–Win) over the Himalayas and the IGP calculated using the 2-tailed student's t-test (unequal variance). p-values ≤ 0.05 shown in boldface

	Aerosol optical depth (AOD)				Ångström exponent (α)			
Location	Win – Pre-M	Pre-M – Mon	Mon – Post-M	Post-M – Win	Win – Pre-M	Pre-M – Mon	Mon – Post-M	Post-M – Win
Himalayas:								
1. Jomsom	**<0.01**	**<0.01**	0.11	0.11	0.72	**<0.01**	**<0.01**	**<0.01**
2. Mt. Everest	**<0.01**	0.08	**<0.01**	**<0.01**	**<0.01**	0.71	**<0.01**	**<0.01**
3. Nam Co	**<0.01**	**<0.01**	**<0.01**	0.48	0.12	0.42	0.79	0.06
Himalayan foothills:								
4. Pokhara	**<0.01**	**<0.01**	0.79	**<0.01**	**<0.01**	**<0.01**	**0.04**	**<0.01**
5. Kathmandu	**<0.01**	**<0.01**	0.21	0.29	0.11	**0.01**	**0.05**	**<0.01**
Western IGP:								
6. Karachi	**<0.01**	**<0.01**	**<0.01**	0.51	**<0.01**	0.21	**<0.01**	**0.03**
7. Lahore	**<0.01**	**<0.01**	0.10	**<0.01**	**<0.01**	**0.04**	**<0.01**	0.15
8. New Delhi	0.46	0.76	0.10	0.27	**<0.01**	**0.03**	**<0.01**	0.28
Central IGP:								
9. Lumbini	**0.01**	**<0.01**	**<0.01**	**<0.01**	**<0.01**	0.18	**<0.01**	0.66
10. Kanpur	0.15	0.15	0.41	0.74	**<0.01**	**<0.01**	**<0.01**	0.44
11. Gandhi College	**<0.01**	0.75	**<0.01**	0.51	**<0.01**	**<0.01**	**<0.01**	**<0.01**
Eastern IGP:								
12. Dhaka	**<0.01**	**<0.01**	**<0.01**	0.16	0.76	0.59	**<0.01**	**<0.01**
13. Bhola	**<0.01**	**<0.01**	0.07	**<0.01**	0.26	**<0.01**	**<0.01**	**<0.01**

in winter and post-monsoon whereas α is about 0.5 during pre-monsoon and monsoon; the higher α arises due to the dominance of fine mode aerosols (urban industrial and biomass burning emissions) and lower α values occur due to the dominance of coarse mode aerosols (dust and sea salt particles). Since, the AODs are nearly constant throughout the year their seasonal variations are statistically insignificant while the α values exhibit significant seasonal variability. As a result, their seasonal variations are statistically significant except for post-monsoon to winter as the respective α values are quite close (Fig. 4; Table 2). These distinct characteristics of AOD and α, and their unique relation are very useful to determine and quantify the aerosol types present over a region (Sect. 4.2, Fig. 5).

Ground-based AERONET observations with respect to MODIS satellite retrieved AODs

The MODIS-retrieved AODs, which show the spatial variations at grid level (Fig. 2), are lower over the study region than the ground-based observations (Fig. 4), and the seasonal signatures are not so remarkably seen as well in MODIS AODs. A systematic and comprehensive co-located validation of AERONET and MODIS AODs over South Asia covering all the seasons revealed that only < 70% of MODIS AODs were within the expected error (EE) envelope (Ansari and Ramachandran 2024) while ≥80% of AODs over North America and Europe were within EE. The expected error envelope provides the percentage of MODIS AODs that lie within ±1σ of the match ups on a scatter plot (for example, drawn between MODIS and AERONET AODs), which is crucial for validation studies. The EE of AOD retrieved from MODIS over land is $\pm (0.05 + 0.15 \times AOD_{AERONET})$ (Levy et al. 2013). The Global Climate Observing System (GCOS) sets out a generalized and stricter observational requirement for the required aerosol data record, which is demanded by the climate modelling community (Popp et al. 2016). For AOD, the GCOS requirement is that the accuracy of AOD should be better than 10% or 0.03 whichever is higher (Popp et al. 2016). In the validation of AOD by models and satellites, the number of valid points is quantified by GCOS fraction (%), which corresponds to the fraction of satellite AODs whose differences with respect to AERONET AOD lie inside the GCOS requirement envelope. The GCOS fraction provides a quantitative measure that is crucial for validating the AODs obtained by satellites and models; the agreementt between observed and satellite derived/model simulated AOD is better when GCOS fraction is higher. The GCOS fraction over South Asia was also less (< 33%), and significantly lower than North America (~ 60%) and Europe (67%) (Ansari and Ramachandran 2024). The higher percentage of AODs within the EE and higher GCOS fraction over North America and Europe arise due to lower AODs (~ 0.2) and negligible seasonal variations in AODs. In contrast, AODs are higher over South Asia and exhibit noticeable seasonal variations (Ansari and Ramachandran 2024), clearly emphasizing the need and importance of such high-quality ground-based observations to document and quantify the aerosol impact on radiation and climate in a more robust manner over South Asia, a highly polluted and complex-aerosol region.

Simulations of aerosol characteristics across Himalayas and IGP: Constraints, challenges, suggestions

It is pertinent to note that these results from AERONET and satellite(s) usefully inform and provide valuable constraints for high-resolution chemistry-transport modelling (which is beyond the scope of the present study) to advance our understanding of aerosols and their radiative and climate impacts over the IGP and the Himalayas. The availability of AERONET data during all the seasons in the year over this region from all the stations simultaneously remains a challenge, and as mentioned earlier, AERONET data were available only for a particular time frame for all the locations in the study region, this lacuna from the observational point of view is addressed in this study. However, it should be mentioned that the GCM/ESM/CTMs that participated in the CMIP6 experiments, the results of which are used in the IPCC 6th Assessment Report (2021) were not able to reproduce the observed magnitudes of AOD over the IGP and the Himalayas (Ramachandran et al. 2022). The high AODs across the IGP, a profound feature of aerosol loading over Asia was missing in most model simulations (Ramachandran et al. 2022). Furthermore, the magnitude of simulated AODs across models differed significantly – AODs were lower in CNRM-ESM2-1, and CESM2 simulations with respect to the model mean and observations, whereas the AODs were a factor of 2-higher in CanESM5 and GISS-E2-1-G simulations compared to the above models (Ramachandran et al. 2022). Further, MODIS AODs were significantly lower than AERONET AODs over the IGP region (Ramachandran et al. 2020). The statistical significance of intra-annual (seasonal) variations in AOD at a particular wavelength (in this case 0.5 μm) and the Ångström exponent (α) vary (similar and dissimilar) both on season and location (Table 2). For example, at the Mt. Everest site, the seasonal variations in AOD and α are statistically significant during winter-pre-monsoon, monsoon-post-monsoon and post-monsoon-winter (Table 2) whereas over Kanpur and Delhi where the inter-seasonal changes are not statistically significant, the inter-seasonal changes in α are statistically significant between winter and pre-monsoon, pre-monsoon and monsoon, and monsoon and post-monsoon, respectively. This

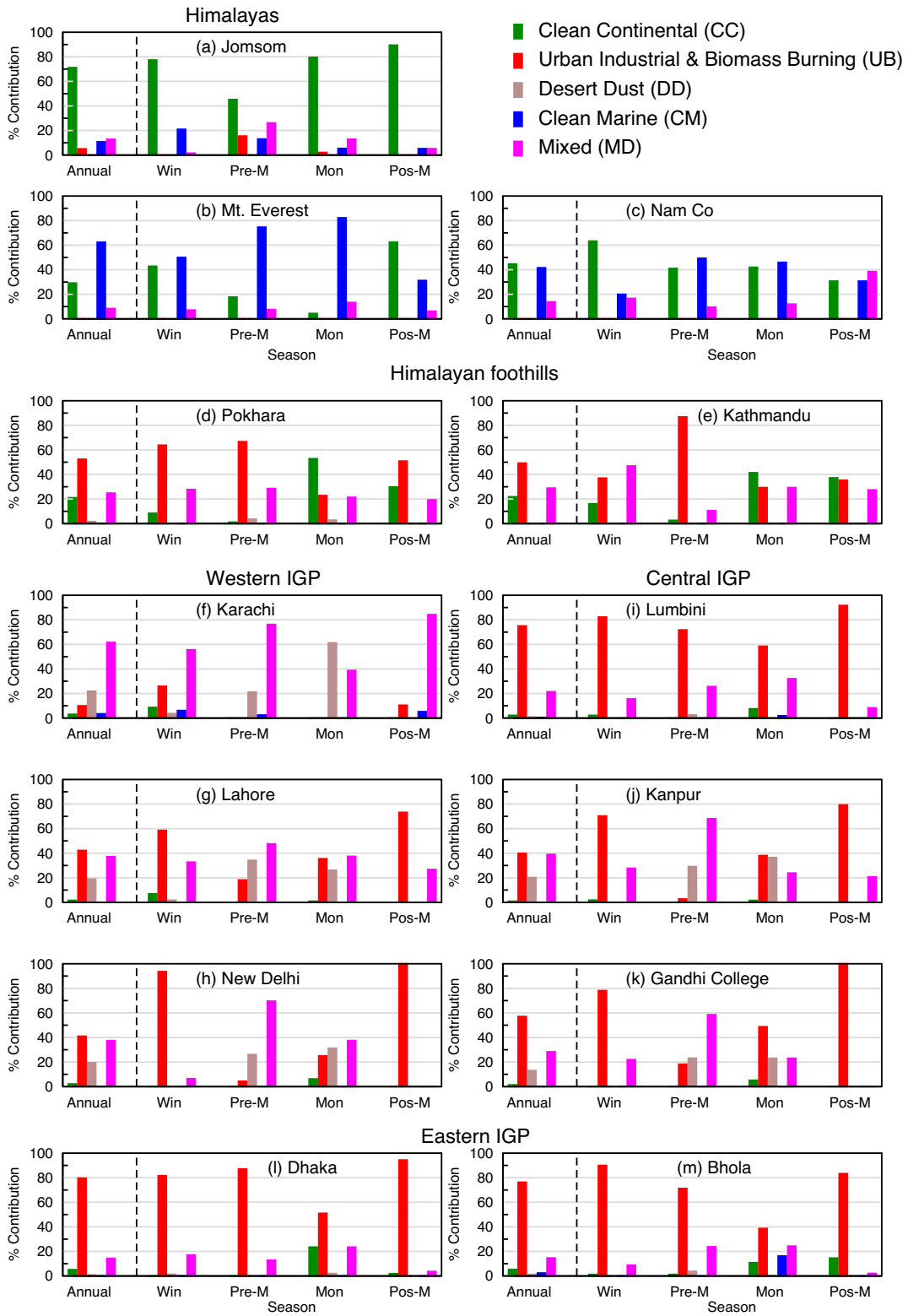

Fig. 5 Aerosol types classified as clean continental (CC), urban industrial and biomass burning (UB), desert dust (DD), clean marine (CM) and mixed (MD) from the relation between AOD and Ångström exponent (α). The percentage contribution of the 5 aerosol types on annual and seasonal mean basis over the study locations in Himalayas ((**a**) Jomsom, (**b**) Mt. Everest, (**c**) Nam Co), Himalayan foothills ((**d**) Pokhara, (**e**) Kathmandu), western IGP ((**f**) Karachi, (**g**) Lahore, (**h**) New Delhi), central IGP ((**i**) Lumbini, (**j**) Kanpur, (**k**) Gandhi College), and eastern IGP ((**l**) Dhaka, (**m**) Bhola)

poses another challenge in simulating the observed aerosol characteristics over the study region as it is crucial not only to simulate well the magnitude of AOD at a given wavelength but also in the entire spectral range in order to estimate the radiative and climate impacts of aerosols more accurately. This is crucial over the study region as both fine and coarse mode aerosols from anthropogenic and natural sources co-exist, and contribute in different proportions to AODs at different wavelengths (Fig. 2). In this context, the results obtained on aerosol characteristics in the present study that is constrained by observations on a seasonal scale are vital for providing observationally-constrained inputs to model simulations.

AODs were found to be underestimated by Model for OZone And Related Tracers (MOZART) and Goddard Global Ozone Chemistry Aerosol Radiation and Transport (GOCART) chemical transport models over South Asia, especially the IGP (Ramachandran et al. 2015). The correlation between observed and simulated AODs was found to be good over Nainital ($r > 0.83$), a free tropospheric site (2084 m above mean level) in the IGP, where the AODs were also lower. These differences between observations and model simulations pointed out the need to improve emission inventories of aerosol sources, and removal mechanisms of aerosols in the models. These attributes were confirmed in later studies conducted over South Asia. For example, during winter season, when AERONET AOD was comparatively higher, the underestimation by MERRA-2 simulation was also higher over the IGP (Gueymard and Yang 2020; Ansari and Ramachandran 2023). In contrast, Copernicus Atmosphere Monitoring Service (CAMS) simulated AOD was always higher than AERONET and MERRA-2, and exhibited higher positive correlation (Gueymard and Yang 2020; Ansari and Ramachandran 2023). Further, the differences between observations and model simulations were found to be the lowest during pre-monsoon as both models perform best during pre-monsoon season when total AOD was relatively smaller and the contribution of fine mode aerosols was lower, whereas during high aerosol loading seasons such as post-monsoon and winter, when anthropogenic emissions and agricultural waste burning emissions dominate, not only the differences between model simulations and AERONET measurements, but also the inter-model differences were higher over the IGP (Ansari and Ramachandran 2023). Over the IGP during winter and post-monsoon, the ABL is shallower and the aerosol emissions are capped near the surface whereas during pre-monsoon and monsoon ABL is deeper when surface aerosol emissions are transported to higher heights. An analysis revealed that the performance of CAMS over the IGP was better due to the recent and updated emission inventories of anthropogenic and biomass burning used in CAMS indicating that the temporal evolution of dominant aerosol sources (SO_2 and BC) is crucial, especially in winter (Ansari and Ramachandran 2023). In addition, a comparison between AERONET and model simulated dust AOD showed differences, especially during pre-monsoon when dust aerosols dominate, emphasizing that parameterization and physical processes related to transport of dust needs to be improved (Ansari and Ramachandran 2023) in models.

In global climate models, and chemical transport models, the simulation of AOD and its spectra is based on the emission inventories of different aerosol species (anthropogenic and natural: sulfate, black carbon, organic carbon, sea salt and dust), their optical properties, and the parameterization schemes for transport, meteorological parameters (relative humidity, atmospheric boundary layer, winds), removal (wet and dry deposition) mechanisms and radiation. Threshold values of AOD and α, along with their respective uncertainties can be effectively utilized in models to derive/constrain more accurate AOD and α values as demonstrated in a sensitivity study later (Section 4.2). Further, threshold values of AOD and α used in the study, for example, can be utilized to calculate the contribution of aerosol types from the models, which can be directly compared on a one-on-one basis with observationally-constrained values derived from AERONET observations (Figs. 4, 5, 6, 7 and 8). The discrepancies identified from such a comparison between modeled and observed aerosol types, and their percentage contributions can provide valuable attributable insights on whether the differences are arising due to the differences (or lack of) in the respective aerosol emission(s), parameterization processes of transport including vertical mixing (e.g., convection/advection of aerosols), and/or their optical properties. Thus, the observations and constraints on physical and optical characteristics of aerosols (AOD, FMF, α, and size distribution) including their types reported in the present study on seasonal scale over an aerosol hotspot can be effectively used as the basis to verify the emission inventories of dominant aerosol sources as a function of season and size, transport mechanism, and parameterization schemes in models, and thereby improve the correlation between observed and model simulated aerosol characteristics, which will enable a more robust and accurate assessment of aerosol radiative and climate effects.

Comparison: Commonality and uniqueness of aerosols over the Himalayan and the IGP environment

There are only a couple of studies on aerosol optical properties in the Himalayan foothills and the mountain region. AODs analyzed in a pre-monsoon campaign conducted in 2009 in the Himalayan foothills - at Hetauda (27.4°N, 85.0°E, 465 m asl) during 18 Apr-30 May, and Dhulikhel 27.6°N,

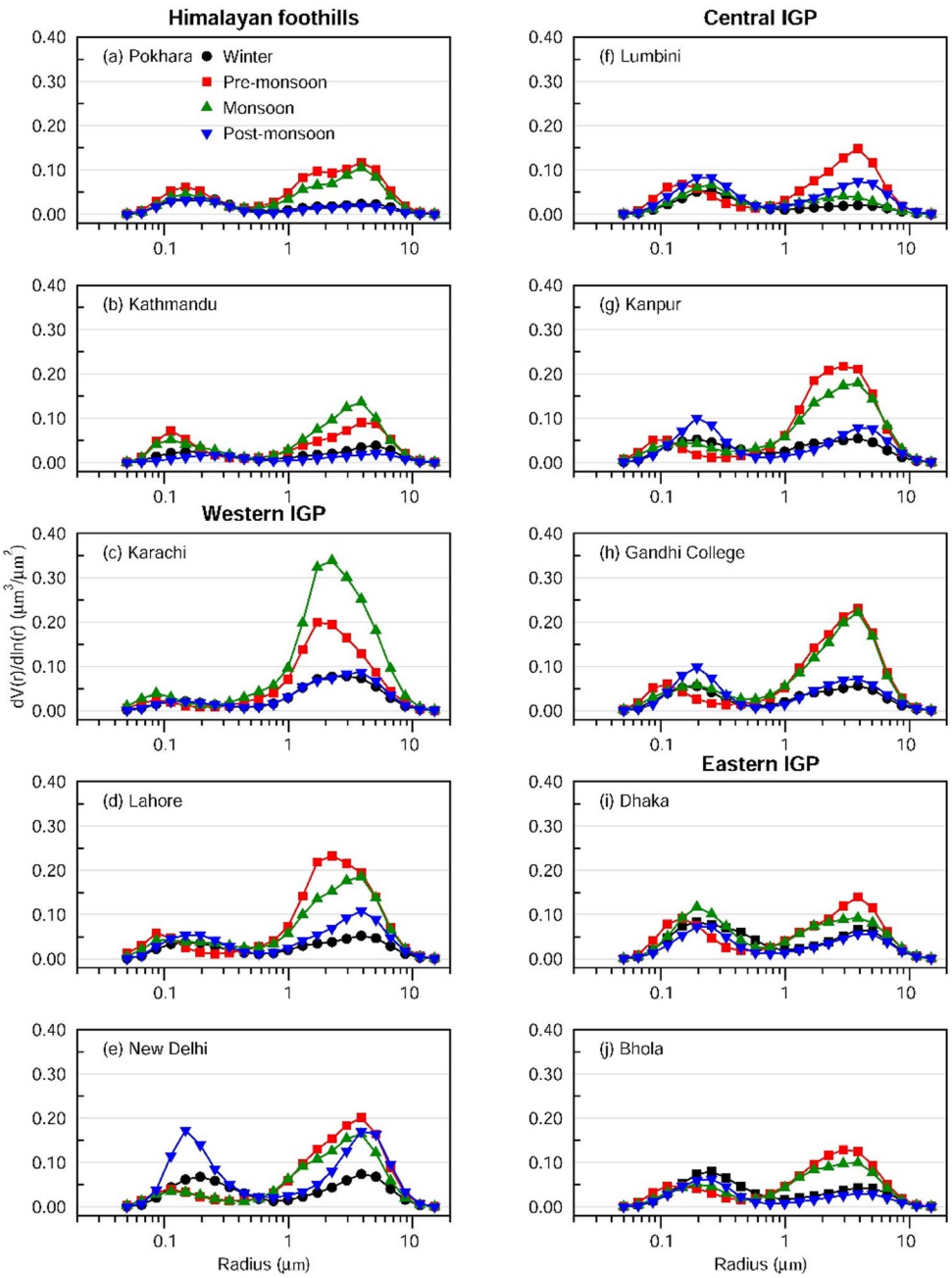

Fig. 6 Seasonal average aerosol volume size distributions in the 0.05 to 15 μm radius range over the study locations in Himalayan foothills - (**a**) Pokhara and (**b**) Kathmandu in Nepal, western IGP – (**c**) Karachi and (**d**) Lahore in Pakistan, and (**e**) New Delhi in India), central IGP – (**f**) Lumbini in Nepal, and (**g**) Kanpur and (**h**) Gandhi College in India, and eastern IGP – (**i**) Dhaka and (**j**) Bhola in Bangladesh

85.5ºE, 1500 m asl) during 11 Apr-16 Jun in Nepal, were reported earlier in Gautam et al. (2011). Hetauda and Dhulikhel AODs were high and quite close at 0.75±0.50 and 0.73±0.49, respectively. No significant difference in AODs were evident as the elevation increased from Hetauda to Dhulikhel. The respective α values for Hetauda and Dhulikhel were 1.10±0.27 and 1.23±0.36. Similarly, the pre-monsoon season AODs in the present study (Fig. 4a) are comparable (~0.73) to them, and do not show significant difference as the altitude increases from Lumbini (110 m), to Pokhara (800 m) and to Kathmandu (1297 m), all in the Himalayan foothills (Fig. 4a). The pre-monsoon α values are however lower over Lumbini, Pokhara and Kathmandu, and also over Jomsom, Nam Co and Mt. Everest (Fig. 4c) than reported in Gautam et al. (2011). The AOD (at a wavelength of 0.675 μm) during pre-monsoon was high (0.63) over Kathmandu and the minimum (0.20) occurred during monsoon (Cho et al. 2017) which is consistent with the features in seasonal AOD variations in the present study (despite the differences in wavelengths of AOD). The α values were lower during pre-monsoon (1.1) and higher during monsoon (1.5–1.6) over Kathmandu during the year which was attributed to the predominant presence of fine mode aerosols throughout the year (Cho et al. 2017) similar to the current results (Fig. 4).

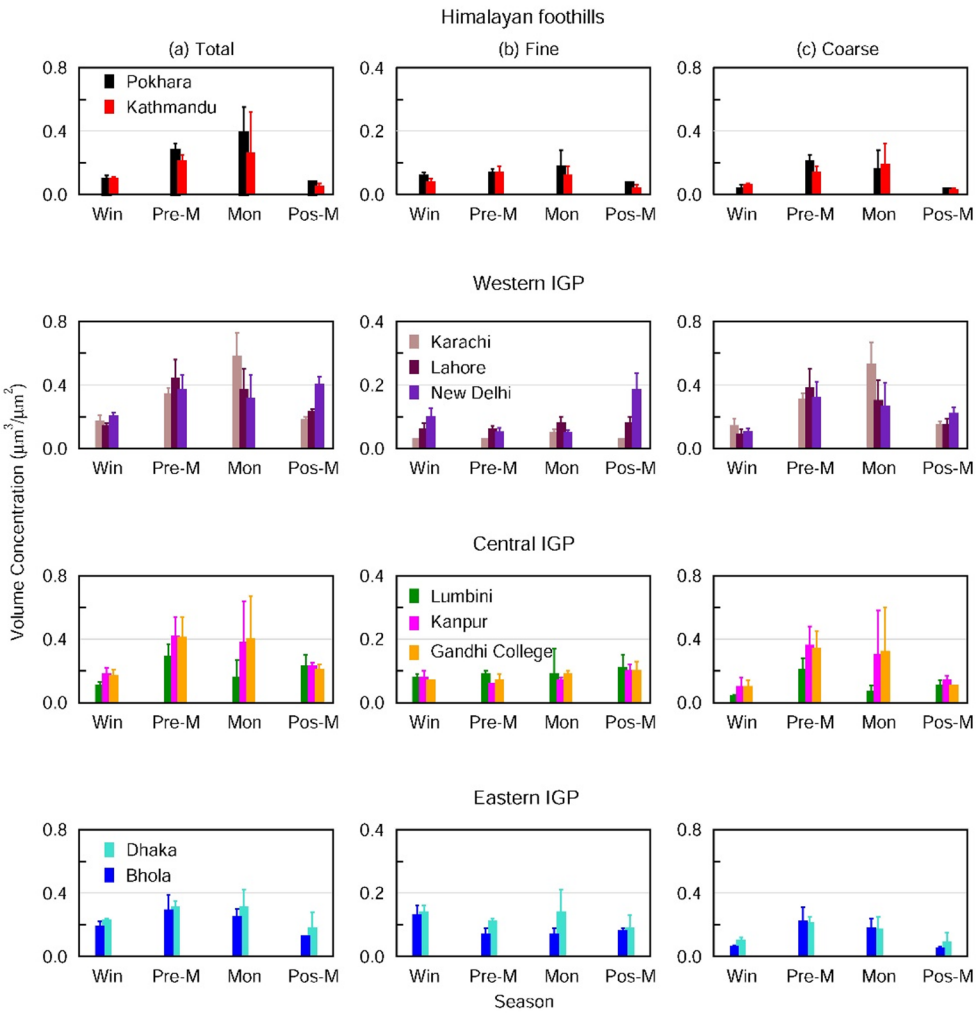

Fig. 7 Volume concentration of (**a**) total (fine + coarse), (**b**) fine, and (**c**) coarse modes in the 0.05 to 15 μm radius range during winter, pre-monsoon, monsoon and post-monsoon over the study locations in Himalayan foothills - Pokhara and Kathmandu in Nepal, western IGP – Karachi and Lahore in Pakistan, and New Delhi in India, central IGP – Lumbini in Nepal, and Kanpur and Gandhi College in India, and eastern IGP – Dhaka and Bhola in Bangladesh. Vertical bars indicate ± 1σ standard deviation from the mean

AERONET retrieved AOD over Dushanbe in Central Asia (38.6°N, 68.9°E, 821 m asl), located in the vicinity of Taklamakan, Karakum, and Aralkum deserts, was > 0.2 for most of the year due to dust aerosols, particularly in summer and autumn (Rupakheti et al. 2020). The annual average AOD was 0.28 ± 0.20, with α at 0.61 ± 0.25 (Rupakheti et al. 2020). FMF values were 0.77 (winter), 0.50 (spring), 0.39 (summer), and 0.50 (autumn) (Rupakheti et al. 2020), with seasonal variations similar to the IGP. Higher FMF and α in winter were attributed to more anthropogenic aerosols, while lower FMF in summer and autumn reflected dust influences (Rupakheti et al. 2020). In Minsk, Belarus (53.9°N, 26.6°E, 235 m asl), the annual mean AOD was lower at 0.22 ± 0.17, with α averaging 1.42 ± 0.29 (Filonchyk et al. 2021), higher than Dushanbe but comparable to the IGP and the Himalayas. These differences were due to the predominance of coarse-mode particles in Minsk's autumn and winter, and fine-mode aerosols in spring and summer (Filonchyk et al. 2021). In comparison, over the IGP and the Himalayas, AOD is higher in winter and post-monsoon than pre-monsoon and monsoon (except Kathmandu, Pokhara and Jomsom where AOD is higher during pre-monsoon) (Fig. 4), with fine-mode aerosols dominating in these seasons (as evident in higher FMF and AE in winter and post-monsoon).

Aerosol types based on relationship between aerosol optical depth and Ångström exponent

The relationship between aerosol optical depth (AOD) and the Ångström exponent (α) is instrumental in identifying the major aerosol types present in the atmosphere. The aerosol types are differentiated using threshold values for AOD and α: clean continental (CC) aerosols with AOD < 0.2, α > 1.0; urban/industrial and biomass burning (UB) aerosols with AOD > 0.3, α > 1.0; desert dust (DD) with AOD > 0.6, α < 0.7; clean marine (CM) aerosols with AOD < 0.2, α < 0.9; and mixed (MD) aerosols not conforming to any of the above (Rupakheti et al. 2020). This approach has been adopted successfully over a wide range of aerosol environments across the globe, including the IGP, Tibetan Plateau, Southeast Asia and Central Asia (Rupakheti et al. 2020 and references cited therein). Further, this relationship between

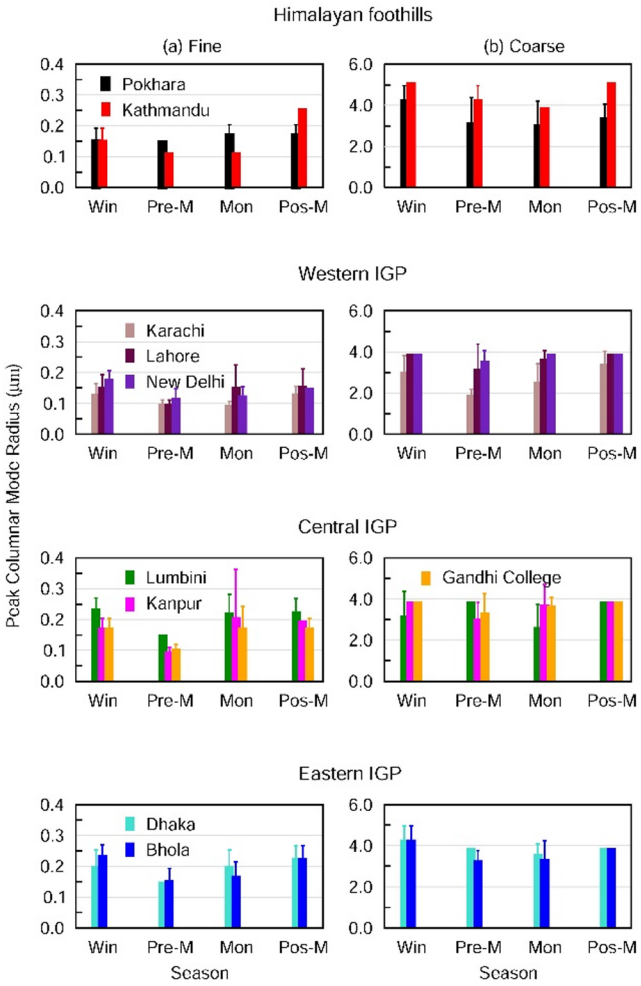

Fig. 8 Peak columnar mode radius (μm) in the (**a**) fine and (**b**) coarse size modes in different seasons over the study locations in Himalayan foothills - Pokhara and Kathmandu in Nepal, western IGP - Karachi, Lahore and New Delhi, central IGP – Lumbini in Nepal, Kanpur and Gandhi College in India, and eastern IGP – Dhaka and Bhola in Bangladesh. Vertical bars correspond to ±1σ standard deviation from the mean

AOD and α has been utilized over many regions across the globe, which have different aerosol sources, emissions, seasonal variations, and atmospheric conditions (Rupakheti et al. 2020 and references cited therein). These studies suggest that the thresholds in AOD and α used to classify the different aerosol types in the atmosphere should be appropriate for South Asia as well. However, in order to determine the appropriateness of these cutoffs for South Asia, a sensitivity analysis was performed, to test how the classification changes with different threshold values. The uncertainty in AERONET AODs is $<\pm 0.01$ for wavelengths >0.44 μm (Holben et al. 2001), and as α is derived using AODs measured at 0.44, 0.50, 0.675 and 0.87 μm by least squares fitting of AOD with respect to wavelength on a log-log plot, it is fair to assume that the uncertainty in α will also be same. The sensitivity analysis was performed for two extreme ranges of AOD and α thresholds: increasing AOD and α thresholds by 10% (AOD+10%, α+10%), and decreasing AOD and α thresholds by 10% (AOD-10%, α−10%) with respect to the above threshold values for different aerosol types (i.e., for clean continental (CC) aerosols with AOD <0.2, $\alpha>1.0$; AOD <0.22, $\alpha>1.1$ (increasing by 10%), and AOD <0.18, $\alpha>0.9$ (decreasing by 10%), and likewise for the other aerosol types). The sensitivity analysis revealed that the changes in classification of different aerosol types are on the order of about ±10% or less over almost all sites in the study region (Himalayas, its foothills, and the IGP) for these two threshold changes, and further, the dominant aerosol type remained the dominant aerosol type even when AOD and α cutoffs changed as above, though their contributions got altered. For example, over Jomsom CC was the most dominant aerosol type (71%) for the initial cutoff of AOD <0.2 and $\alpha>1.0$ which decreased by 6% to 65% for AOD+10%, α+10% whereas the CC contribution increased by 2% to 73% for AOD-10%, α−10% scenarios, respectively. Thus, it is clear from the analysis that changing the thresholds in AOD and α, will mostly affect the dominant aerosol type and not the less dominant aerosol types, and that these changes (increase/decrease) in the dominant type get added/removed to/from the mixed aerosol type. The changes in cutoffs were taken to be quite high (as the uncertainty in AOD and α are significantly less) only for the purposes of this sensitivity analysis and even so the changes in classification of aerosol types are ~10% or less, thus, demonstrating the appropriateness of the above cutoffs in AOD and α used in the present study for South Asia.

Over the IGP and the Himalayas, aerosol types exhibit significant seasonal and spatial variations (Fig. 5). In the Himalayan Mountain region, CC aerosol type (low AOD, $\alpha>1$ (Fig. 4)) is dominant over Jomsom, almost throughout the year, except during pre-monsoon when other aerosol types (UB, CM and MD) are also present. CM (low AOD, $\alpha<1$) dominates over the Mt. Everest region, with seasonal variations - CM peaks during monsoon and declines in post-monsoon, where CC aerosols become prominent. (Fig. 5). In Nam Co both CC and CM aerosol types each contribute 40% annually, with CC dominant in winter. In the Himalayan foothills, UB aerosol type dominates (≥50%) over both Pokhara and Kathmandu, consistent with higher AODs (>0.3) and higher α (>1) (Fig. 4). The atmosphere over the Himalayan foothills (Pokhara and Kathmandu) is dominated by UB and MD aerosol types in winter and pre-monsoon and in pre-monsoon over Kathmandu UB type alone contributes $>85\%$ (Fig. 5), when AOD and α are significantly higher (Fig. 4). MD aerosol type is prevalent year-round over both locations, contributing, on an average, ≥25%, except during winter and pre-monsoon in Kathmandu

where its contributions are >45% and 11%, respectively. It is important to note that DD aerosol type is negligible over the Himalayas and its foothills (Fig. 5), as evident in α values which are never lower than 0.7 in these five locations.

Regarding the IGP sites, on an annual scale, UB aerosol type is higher over all the locations in western, central and eastern IGP except in Karachi and Lahore (Fig. 5). In the western IGP (Karachi, Lahore and New Delhi), UB and MD aerosol types are dominant. MD contributes 60% over Karachi, and MD and UB each contribute ~ 40% over Lahore and New Delhi (Fig. 5). Karachi, being a sea port and an urban area, which is influenced by dust experiences high amount of mixed aerosols during the year, however, the mix of aerosols differ on a seasonal scale; for example, during winter the mix is of UI and DD (Fig. 3c) whereas during post-monsoon the mix is of UI and CM. In comparison, over the Himalayan foothills the MD type is mostly a mix of UB, and CC (especially during monsoon) (Figs. 3 and 5). DD aerosol type is found during pre-monsoon and monsoon over these locations, characterized by higher AOD and lower α (Fig. 4). In New Delhi, UB aerosol type strongly dominates (>94%) in winter and post-monsoon (Fig. 4) due to increased agro-residue burning (more active in post-monsoon) and anthropogenic emissions (Jethva et al. 2018). In winter, in addition to the transport, the regional meteorological conditions over north India (lower temperatures and ABL) favor accumulation of anthropogenic fine mode aerosols (fossil fuel, biofuel and biomass combustion associated emissions including from residential heating) resulting in higher AODs and α (Ramachandran et al. 2015, 2020). DD aerosol type is negligible over Lumbini, located in the northern edge of central IGP, similar to the sites in the Himalayas. DD aerosol type shows more significant variations over western and eastern IGP – it is maximum during monsoon over Karachi; it is more or less the same during pre-monsoon and monsoon over Lahore and Kanpur. The DD aerosol type is present during pre-monsoon and monsoon over Gandhi College albeit with a lesser magnitude confirming that there exists a gradient in dust over the IGP as we travel from west to east, which is consistent with the transport pathways and probable source regions (Fig. 3). DD aerosol type contribution is insignificant during winter and post-monsoon over western and central IGP, and over eastern IGP the contribution of DD aerosol type is negligible throughout the year (Fig. 5). Over Dhaka and Bhola in eastern IGP, UB aerosol type dominates (>70%) during the year and CM aerosol type is present only during monsoon over Bhola, an island station (Fig. 5). This analysis highlights the dominant aerosol types and their seasonal variations across the IGP and the Himalayan region, providing critical insights into their aerosol environments, thus far not available.

In Dushanbe, central Asia, MD (AOD < 0.6, 0.1 < α < 1.5) was the most prominent aerosol type (57%) followed by CC (17%), CM (16%), UB (8%), and DD (<3%) (Rupakheti et al. 2020). Despite being located in a desert-influenced region, DD had minimal contribution. Seasonal variations showed MD peaking up in summer (>70%) and CC reaching ~ 40% in winter (Rupakheti et al. 2020). In Minsk, Belarus's most densely populated and industrialized city, CC dominated (>50%) followed by MD (24%), UB (21%) CM (3%), and DD (<1%) (Filonchyk et al. 2021). CC prevailed across all seasons, peaking in winter and autumn (59%), and decreasing in summer (51%) and spring (49%) (Filonchyk et al. 2021). MD was present year-round, highest in summer (27%) and lowest in winter (16%) (Filonchyk et al. 2021). Whereas, the MD aerosol type dominates over the Himalayan foothills and the entire IGP (Fig. 5), confirming that mixed-type aerosols prevail in the regions influenced by both fine-mode anthropogenic aerosols and coarse-mode natural aerosols. DD aerosol type contribution is negligible over the Himalayas during the year (Fig. 5). Further, similar to Dushanbe and Minsk, DD aerosols are negligibly small or absent in winter and post-monsoon seasons across the Himalayan foothills, and IGP sites (Fig. 5). However, DD aerosols are detected in the western and central IGP, predominantly during the pre-monsoon and monsoon seasons (Fig. 5). The variations and percentage contributions of aerosol types across the Himalayas and the IGP differ and are unique in comparison to these locations – CC type is highest over the Himalayas followed by the Himalayan foothills, revealing a commonality of aerosols between the Himalayas, Minsk and Dushanbe, at the same time the contribution of CC aerosol type is negligible over the entire IGP (western, central, and eastern) demonstrating the intra-regional variability of dominant aerosol types and a gradient across the Himalayas and the IGP from a cleaner to a polluted region.

Size distribution, volume concentration, and effective radius

As mentioned earlier the inversion products were not available for three high altitude sites, we present here the size distribution, volume concentration, volume mean radius and effective radius for the remaining ten sites. The aerosol volume size distributions are bimodal – with a modal radius in the 0.10–0.30 μm range corresponding to fine mode (0.05–1.0 μm), and the other mode lying between 2 and 5 μm in the coarse mode (1.0–10.0 μm) (Fig. 6). The retrieval of VSD was proven to be satisfactory for all AOD values > 0.05 in different aerosol environments (urban/industrial, mixed, biomass burning, desert and maritime), and the volume size distributions had low values at the edges of retrieval size

interval (beyond 0.05 and 15 μm) (Dubovik et al. 2002). The AERONET retrieved VSDs showed good agreement with VSDs derived from data obtained using other techniques/instruments (optical particle counter and nephelometer) (Dubovik et al. 2002). The retrieved VSD was always bimodal (Fig. 2, Dubovik et al. 2002) and the median size of fine mode increased with increase in AOD (Dubovik et al. 2002). For example, over GSFC, Maryland, an urban/industrial aerosol environment, the fine mode radius increased from 0.12 μm for an AOD of 0.04 to 0.21 μm for an AOD of 0.9 (Dubovik et al. 2002). The volume concentrations at the peaks were ~0.01 $\mu m^3/\mu m^2$ and ~0.15 $\mu m^3/\mu m^2$, respectively (Dubovik et al. 2002). An increase in the median radius of the coarse mode with increase in AOD was also observed over urban and biomass burning sites, however, the increases were minor and were comparable to the retrieval accuracy levels (Dubovik et al. 2002). A bimodal volume size distribution throughout the year can occur due to the mixing of air masses containing aerosols in fine and coarse modes and/or due to nucleation, accumulation and growth of aerosols through gas-to-particle conversion mechanism. In addition, the volume size distributions also depend on emission sources, composition, transportation and removal mechanism (Eck et al. 2010). The following features are evident from the size distributions - (a) fine mode volume concentration is equal to or higher than coarse mode volume concentration during post-monsoon and winter, (b) coarse mode volume concentration is higher than (about twice) (or comparable to) fine mode volume concentration during pre-monsoon and monsoon, (c) volume concentrations are a factor of 2-higher over Karachi and Lahore when compared to the other locations, and (d) the coarse mode volume concentrations over Karachi and Lahore are a factor of 4 higher when compared to the fine mode volume concentrations. Over New Delhi the impact of transport of aerosols emitted by strong agro-residue burning during post-monsoon season (Jethva et al. 2018) on the aerosol volume size distribution is evident – the concentrations in fine mode increased at least by a factor of 3 than the other seasons, as a result of which the aerosol type was only UB (100%) (Fig. 5). In general, the emissions from agro-residue burning are in the fine mode size, however, the coarse mode volume concentrations also have increased significantly due to aging, processing, transformation and mixing with urban aerosols and smoke particles during transport. The volume concentration gradually increases from winter to monsoon. Over all the locations the coarse mode volume concentration increases considerably during MAM and JJAS, the pre-monsoon and monsoon seasons, respectively. The increase is significantly higher over locations such as Karachi, Lahore, New Delhi, Kanpur and Gandhi College, as all these sites are more strongly influenced by a significant increase in the dust, and Karachi by sea salt aerosols as well in these seasons. The coarse mode particle concentration increases at the other locations as well (Fig. 7). The coarse mode concentration dominantly contributes (>75%) to the total volume concentration during pre-monsoon and monsoon, especially in Karachi, Lahore, New Delhi, Kanpur and Gandhi College. Among Karachi and Lahore, the coarse mode concentrations are close to each other in MAM (pre-monsoon) whereas during JJAS (monsoon) the coarse mode concentration over Karachi is significantly higher, as it is a coastal location influenced by dust and sea salt aerosols.

The modal radii of fine mode (r_f) and coarse (r_c) mode at which the aerosol volume concentration peaks (Fig. 6) also show significant regional and temporal variations (Fig. 8). In the foothills of the Himalayas the r_f is lower for Kathmandu than Pokhara, during pre-monsoon and monsoon. The Kathmandu r_f is higher during winter and post-monsoon. The r_c is higher (by >1 μm) during post-monsoon and winter over Kathmandu than Pokhara, and remain same during other two seasons. The increase in r_c in Kathmandu during ON and DJF, the post-monsoon and winter seasons, respectively are attributed to coarse soil particles from unpaved roads and farmlands (Cho et al. 2017), as sea salt which is in coarse mode does not contribute significantly over this region (Tripathee et al. 2017). Among all study locations r_f and r_c over Karachi are the lowest during DJF, MAM and JJAS (Fig. 8), while during ON r_f is lower than other sites and r_c is comparable to other sites. As Karachi is a densely populated urban area with two seaports, the freshly emitted urban aerosols get mixed with dust and sea salt particles (the time available to age, process and transform is less for these aerosols) (the mixed aerosol type is the most prominent, Fig. 5), and give rise to smaller modal radii in both fine and coarse modes. This is a unique feature in Karachi can be seen by comparing the values with Lahore, in the same region, where r_f is the same for both cities only during pre-monsoon, while during the remainder of the year r_f and r_c are higher over Lahore. The r_f and r_c over New Delhi, another site in western IGP are mostly similar to Lahore, Kanpur, and Gandhi College. Among the sites in central IGP, Lumbini has significantly higher r_f in all seasons, r_c is nearly the same for all sites in post-monsoon and winter, and r_c is almost 1 μm smaller for Kanpur in pre-monsoon and for Lumbini in monsoon. Though r_c is lower over Kanpur during pre-monsoon, the volume concentrations in the 2–4 μm radius range are comparable – the Kanpur volume distribution is broader as compared to New Delhi which exhibits a sharp peak (Fig. 6e) and Gandhi College, and Lumbini. The higher r_f of aerosols in Lumbini could be due to the presence of cement dust throughout the year emitted from a number of cement factories in Lumbini area, as cement dust typically has bimodal size distribution with a fine mode

at 0.1–0.4 μm and a coarse mode at 1.0–5.0 μm (Liu et al. 2019). Over New Delhi during post-monsoon because of the transport of aerosols emitted by strong agricultural residue burning (Jethva et al. 2018) the fine and coarse mode concentrations are same. In eastern IGP, r_f over Dhaka is lower than Bhola in winter and higher in monsoon; r_f values are the same during pre- and post-mon over both locations. The r_c values are also same except during pre-monsoon when it is higher over Dhaka perhaps due to the differences in the shape of the distribution – sharper in Dhaka and flatter over Bhola.

In Dushanbe, the fine-mode modal radius peaked at 0.09 and 0.11 μm, shifting to larger sizes in winter, while the coarse-mode peaked at 3.86 μm, shifting to smaller sizes (<2 μm) in spring (Rupakheti et al. 2020). Coarse-mode concentrations were significantly higher (3–4 times) in summer and autumn due to coarse dust particles (Rupakheti et al. 2020), similar to the IGP and the Himalayas during pre-monsoon and monsoon seasons (Fig. 7). In Minsk, the volume size distribution (VSD) was bimodal with modal radius at 0.11–0.19 μm (fine) and 3.86–5.06 μm (coarse) (Filonchyk et al. 2021). They are similar to the fine-mode and coarse-mode modal peaks observed over the IGP and the Himalayas. VSD patterns over Dushanbe resembled those of the IGP and the Himalayan foothills – the peak fine mode concentrations were $<0.04\ \mu m^3/\mu m^2$ during the year, the coarse mode concentrations in winter and spring were also $\leq 0.04\ \mu m^3/\mu m^2$, whereas the peak coarse mode concentrations were ~0.12 and $0.16\ \mu m^3/\mu m^2$ in autumn and summer, respectively (Rupakheti et al. 2020). In comparison, the IGP and the Himalayan foothill locations had higher or comparable aerosol concentrations in both modes than those observed in Dushanbe - peak fine-mode concentrations at these South Asia sites of $>0.05\ \mu m^3/\mu m^2$ during the year, and the peak coarse-mode volume concentrations going up to at least $20\ \mu m^3/\mu m^2$ in Kanpur, Karachi, Gandhi College, Lahore, and New Delhi. The relatively higher concentrations of aerosols in both fine and coarse modes over the IGP and the Himalayan foothill locations than Dushanbe result in higher AODs at these South Asian sites. In contrast, Minsk (Fig. 4, and Filonchyk et al. 2021) had significantly lower aerosol volume concentrations in both modes than the IGP, the Himalayan foothills and Dushanbe. The fine-mode volume concentration peaks at Minsk are at ca. $0.02\ \mu m^3/\mu m^2$ and the coarse-mode concentration peaks are at around $0.02\ \mu m^3/\mu m^2$ or less. Fine-mode concentrations here exceeded coarse-mode concentrations in all seasons except winter. The volume size distribution in winter over Minsk differs (lower) from other seasons because fine-mode modal radius shifts from ca. 0.15 μm in other seasons to a larger radius of 0.19 μm in winter (Filonchyk et al. 2021). The increase in fine-mode particles in Minsk during summer and spring was attributed to hygroscopic growth of aerosols due to high RH (Sect. 2), while rise in coarse-mode particles during spring and autumn was linked to increased agricultural activities. The decrease in coarse-mode particles in summer was due to wet removal (Filonchyk et al. 2021).

The volume mean radius (VMR or the mean logarithm of radius) is seasonally and spatially less variant across the IGP and the Himalayan foothills (Fig. 9). The coarse mode VMR is 10-times higher than the fine mode VMR over all locations (Fig. 9). The total VMR (for the entire volume aerosol size distribution in the 0.05–0.15 μm radius range) is smaller as it corresponds to a combination of fine and coarse mode VMR. The variations seen earlier in the peak modal radii in fine (r_f) and coarse (r_c) modes (Fig. 9) are very well captured by VMR. The seasonal pattern in fine and coarse mode VMR obtained over Kanpur (present study) during 2012 are similar to that obtained during 2001–2003 (Singh et al. 2004), however, our values are higher than those obtained during 2001–2003, suggesting that both fine and coarse mode radii have increased during the previous 2-decades over the IGP region.

The effective radius (r_e) is defined as the ratio between the total volume of the aerosol size distribution and the surface area. The fine mode r_e is <0.25 μm whereas the coarse mode r_e is higher by an order of magnitude across the IGP and the Himalayan foothills (Fig. 10). A relative increase in larger particle concentration in an aerosol size distribution results in higher r_e. The r_e of fine mode aerosols is similar (0.1–0.2 μm) during the year, whereas the coarse mode r_e decreases gradually from DJF (winter) to JJAS (monsoon) and increases again in ON (post-monsoon) because of the associated increase in coarse mode volume concentrations (Figs. 6 and 10). The r_e of total aerosols increases significantly during monsoon at all sites as compared to the other seasons due to a considerable increase in the coarse mode volume concentration (which lowers the α value and the FMF), which is prominently visible in case of Karachi. The AOD, FMF and α (Fig. 4) are compatible with features seen in aerosol size distribution. The volume size distributions obtained over the IGP and the Himalayas compare well with Ilorin in Nigeria, Kanpur in India and Beijing in China, which are also influenced by the same aerosol sources in fine and coarse modes (Eck et al. 2010). The size distribution, concentration and radii over the IGP and the Himalayan foothills (Fig. 10) show the aerosol characteristics that correspond to regions that are influenced by emissions from urban/industrial and biomass burning, dust, and their mixture. The volume in fine mode is higher than coarse mode volume when urban/industrial, mixed and biomass burning emissions influence aerosol distribution (Dubovik et al. 2002) similar to ON and DJF (Fig. 10), and the volume in coarse mode is higher than fine mode when dust dominates

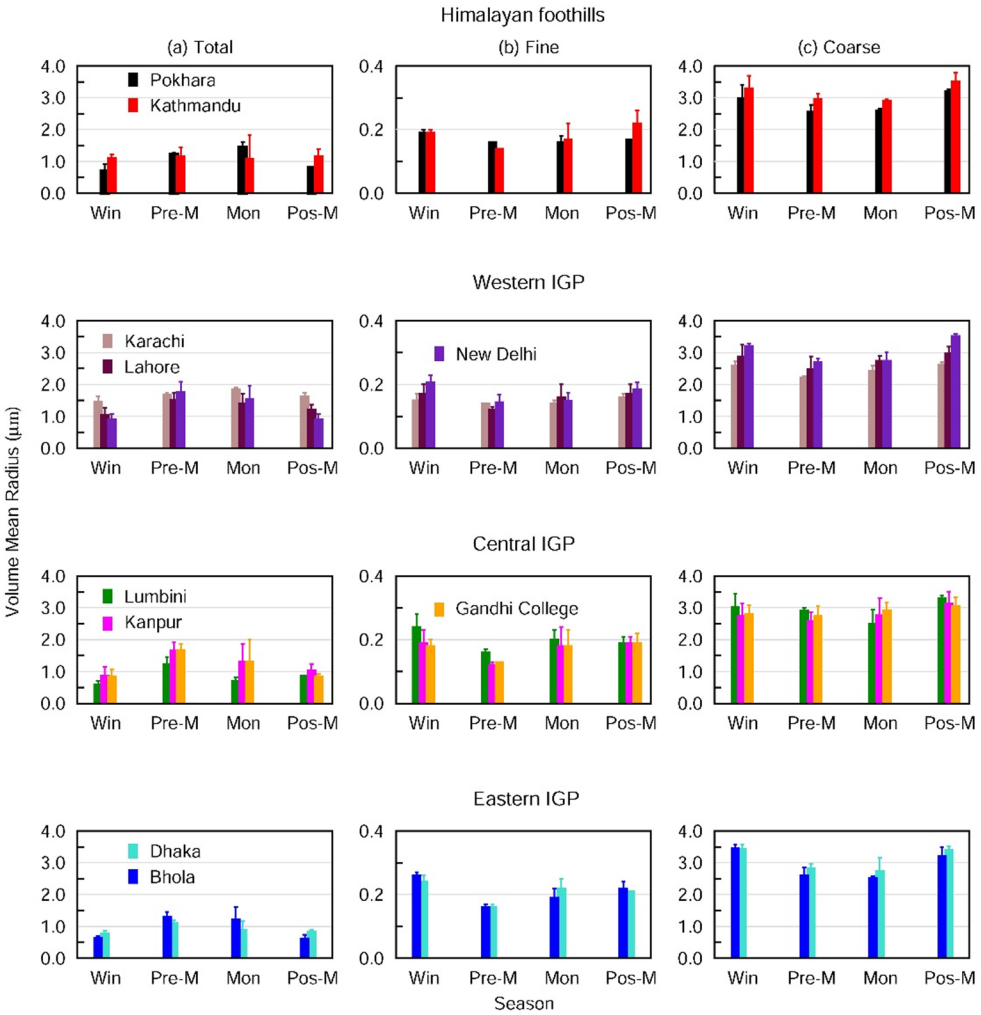

Fig. 9 Volume mean radius (μm) for the (**a**) total (fine + coarse size ranges), (**b**) fine and (**c**) coarse size ranges during different seasons of the year over the Himalayan foothills - Pokhara and Kathmandu, western IGP – Karachi, Lahore and New Delhi, central IGP – Lumbini, Kanpur and Gandhi College, and eastern IGP – Dhaka and Bhola. Vertical bars correspond to ± 1σ standard deviation from the mean

as seen during MAM, in the present study. The coarse mode r_e is lower over a dust dominant region (2.3–2.5 μm) than an urban/industrial and biomass burning aerosol dominant region (r_e = 3.0–3.3 μm). Whereas, r_e in fine mode in all environmental regimes is quite similar (r_e = 0.11–0.15 μm) (Dubovik et al. 2002). These seasonal and spatial features, differences and similarities, in aerosol size distribution, volume concentration and effective radii can be utilized to represent better the aerosol characteristics including at high altitude locations over this regional aerosol hotspot, thereby, improving the characterization/parameterization of aerosol properties in regional and global climate models.

Implications to air quality and climate

The quantitative findings on seasonal variations of physical and optical characteristics of aerosols including the dominant aerosol types from the present study have implications to air quality and climate. The air pollution in South Asia was quite severe with an estimated 13–22% of deaths in this region related to the health effects of air pollution exposure (World Air Quality Report 2020). Air quality or visibility, a measure of level of air pollution is not only a primary public health concern but is equally important in the context of aerosol-climate interaction as the composition of particles present can influence the physical and optical properties of aerosols (e.g., AOD and size). To assess the radiative and climate impact of aerosols, knowledge on the columnar amount (AOD) of aerosols and its space-time variation is crucial. Across the IGP, $PM_{2.5}$ (particulate matter of diameter less than 2.5μm) concentration showed an increasing trend along with a reduction of surface wind speed (Paulot et al. 2022), thereby, worsening the air quality during winter. As the aerosols are confined within the first few km from the surface during winter (Ramachandran 2018) over the IGP especially, and along with slower winds in the lower atmosphere intensify the trends in AOD (Ramachandran et al. 2020). Further, over the IGP stagnation (that occurs due to lack of precipitation, low surface winds, shallow ABL and limited vertical mixing (lower ventilation coefficient) of air pollutants in winter leads to an increase in $PM_{2.5}$ concentrations (Zhou et al. 2024). A systematic analysis of columnar

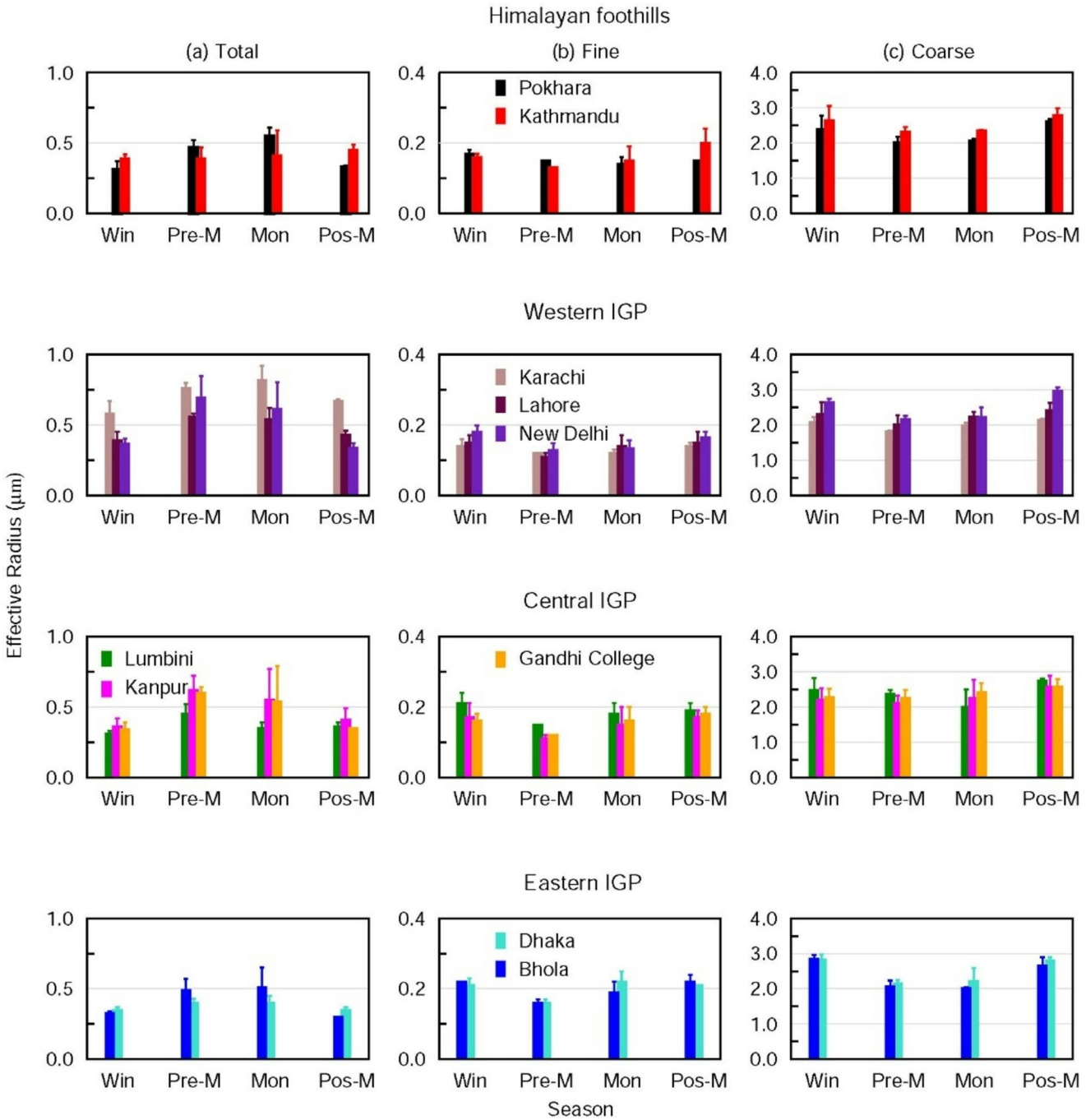

Fig. 10 Seasonal average effective radius (μm) for (**a**) total (fine and coarse size ranges), and for (**b**) fine and (**c**) coarse mode size ranges separately over the study locations – Pokhara and Kathmandu in Himalayan foothills, Karachi, Lahore and New Delhi in western IGP, Lumbini, Kanpur and Gandhi College in central IGP, and Dhaka and Bhola in eastern IGP. Vertical bars represent ± 1σ standard deviation from the mean

AODs and their variations over the pollution hotspot can offer insights on mitigation strategies and reduction in aerosol pollution, as the corresponding relationship between the variation in the range of AODs and air quality is almost linear, i.e., air quality (visibility) improves as the atmospheric loading of particulate matter decreases and vice versa (Li et al. 2020; Cao et al. 2021). For example, in China, in order to improve ambient air quality a series of laws and regulations were issued in the last decade, including the Air Pollution Prevention and Control Action Plan in 2013 and comprehensive three-year (2018–2020) action plan in 2018 (Li et al. 2020). Results showed that the Beijing's air quality had

shown a noticeable improvement over 2013–2019 (Li et al. 2020). SO_2 emissions in Beijing decreased, along with changes in energy structure due to a significant decrease in coal consumption and increase in the consumption of natural gas and electricity (Li et al. 2020). The substantial reduction in coal emissions is found to have played a key role in improving Beijing's air quality (Li et al. 2020). It was suggested that vehicle emission control should be further enhanced. The improvements in air quality over Beijing due to the above reduction in emissions showed the effectiveness of the clean air action plans which have potential implications for other areas and regions which experience severe air pollution (Li et al. 2020). The $PM_{2.5}$ and SO_2 emissions decreased by ~53% and ~85% respectively in 2019 with respect their 2013 values (Li et al. 2020), which are consistent with the decrease in AOD over Beijing during this period (Ramachandran et al. 2020). The rapid and contrasting changes in aerosol loading on intra-regional scale, may result in climate effects that are noticeable over Asia and beyond, which include changes to mean and extreme temperature, precipitation, the onset and strength of the monsoon, availability of freshwater and changes to air quality (Samset et al. 2019). The knowledge on the aerosol amount, types and their seasonal variations over this highly polluted region can further help in devising mitigation measures and stringent air quality restrictions aimed at reducing a particular aerosol type and associated emissions with implications to air quality, environment, human health and climate.

Conclusions

Using new and high-quality columnar aerosol observations, a detailed comprehensive regional analysis of seasonal variations of all key columnar optical (content) and physical (size) properties, crucial in the context of climate change, over the large region comprising the IGP and Himalayas (including a site in southern Tibetan Plateau) is carried out, for the first time. The aerosol optical depth (AOD) in the entire year is ≥0.3 over this region except at the elevated locations situated at >2500 m in the Himalayas and Tibet, confirming that the entire region is heavily polluted. AODs are a factor of 2 to 3 lower at the high altitude sites in the Himalayas. The AODs decrease as altitude increases in general, and remains almost the same beyond 4000 m asl in the Himalayas. During pre-monsoon, both agricultural fires and forest fires, coupled with the regional-scale advection of continental aerosols from polluted regimes, result in higher AODs. During monsoon the transport and the emissions from forest fires get suppressed due to rain; further, major seasonal sources such as brick production are less active in monsoon, leading to AODs of lesser magnitude over the IGP and at elevated locations in the Himalayas. The aerosols in the fine mode (r < 1 μm) (represented by the fine mode fraction (FMF)) contribute > 80% to AOD during ON and DJF months, post-monsoon and winter seasons, respectively, and their contribution decreases during MAM and JJAS months of pre-monsoon and monsoon seasons, respectively, over Lumbini, Pokhara and Kathmandu. The FMF in the high altitude locations of the Himalayas is lower than the sites in the foothills (but FMF is still > 50% throughout the year). This occurs because the aerosols in fine mode from emissions of fossil fuel and biomass burning, which are transported from urban regions are higher near the surface and their contribution to the total AOD decreases as the altitude increases, and in addition at the elevated locations the coarse mode particles (dust) from the local and dry barren lands are expected to be present resulting in lower FMF. The Ångström exponent α, a measure of the spectral dependence of AODs in the 0.44–0.87 μm wavelength region, is consistent with FMF variations. An analysis of aerosol types determined from the relation between AOD and α revealed significant seasonal and spatial variations over the study region. The Himalayan locations are dominated by clean continental and clean marine aerosol types. The atmosphere over the Himalayan foothills is dominated by urban/industrial and biomass burning aerosol types. Dust as an aerosol type is not present over the Himalayas including its foothills. The urban/industrial and biomass burning aerosol type is the most dominant over western, central and eastern IGP except in Karachi and Lahore where mixed aerosol type is significant. This analysis on quantification of dominant aerosol types determines the aerosol environment that characterizes each location over the Himalayas and the IGP.

The aerosol volume size distributions are bimodal in all four seasons, with peaks in fine (0.1-<0.3 μm) and coarse (2–5 μm) modes. The effective radius (r_e) in fine mode remains more or less same (< 0.25 μm) during the year, whereas coarse mode r_e decreases gradually from winter to monsoon. The modal radii of fine (r_f) and coarse (r_c) mode aerosols, at which the aerosol volume concentration peaks show significant regional and temporal variations, and the volume mean radius corroborate the features seen in r_e. These results from a most comprehensive analysis to date, of the optical and physical characteristics across the spatial and temporal scales over a large spatial domain and an aerosol hotspot including high altitude locations in a complex topography, based on high quality observations, heretofore not available, should be used in conjunction with high-resolution chemistry-transport modelling to advance scientific understanding of air pollution (aerosols) over the IGP and the Himalayas to further improve the assessment of aerosol impact on climate in a more certain manner. A comparative analysis of aerosol characteristics revealed

the commonality of aerosols between Himalayas, Minsk (Belarus) and Dushanbe (Central Asia), while at the same time demonstrating intra-regional variability of dominant aerosol types that is unique to Himalayas and IGP, which provide valuable constraints for high-resolution chemistry-transport modelling, inputs to improve satellite retrievals, and help deepen understanding of aerosol impacts on climate and ecosystems in this region. Further, this knowledge on the aerosol amount, types and their seasonal variations over this highly polluted region can help in devising mitigation measures and stringent air quality restrictions aimed at reducing a particular aerosol type and associated emissions with implications to air quality, environment, human health and climate.

Acknowledgements We thank the principal investigators for their efforts in establishing and maintaining the AERONET sites (https://aeronet.gsfc.nasa.gov/) in the IGP and the Himalayas from which data are used in the study. Maheswar Rupakheti acknowledges Brent N. Holben, NASA for providing two sets of CIMEL Sun-photometers for setting up at Bode (Kathmandu Valley) and Lumbini in Nepal. Maheswar Rupakheti setup and maintained the AERONET sites at Kathmandu and Lumbini. The wind data are downloaded from the Physical Sciences Division, Earth System Research Laboratory, NOAA, Boulder, Colorado, from their Web site at http://www.esrl.noaa.gov/psd/. MODIS Terra version 6.1 monthly Combined Dark Target and Deep Blue Land and Ocean AOD at 0.55 µm, monthly Dark Target Land Only AOD at 0.55 µm at 1° resolution (Fig. 2) are downloaded from https://giovanni.gsfc.nasa.gov/giovanni/. We acknowledge the MODIS mission scientists and associated NASA personnel for the production of the data used in Fig. 2. We gratefully acknowledge the NOAA Air Resources Laboratory (ARL) for the provision of the HYSPLIT transport and dispersion model and READY website (https://www.ready.noaa.gov) for the air mass back trajectories drawn in Fig. 3. We thank Kamran Ansari for downloading and plotting the airmass back trajectories for the study region, and for his help in analyzing the data required to draw Fig. 5, and in calculating the statistical significance of seasonal variations in aerosol characteristics (Table 2).

Author contributions **S. Ramachandran**: conceptualization, methodology, data curation, formal analysis, visualization, writing - original draft, review and editing. **Maheswar Rupakheti**: conceptualization, writing - review and editing.

Funding Research Institute for Sustainability at GFZ Helmholtz Centre for Geosciences (RIFS), formerly Institute for Advanced Sustainability Studies (IASS), is funded by the German Federal Ministry Research, Technology and Space (BMFTR) and the Brandenburg State Ministry for Science, Research and Culture (MWFK). This work was performed when S. Ramachandran was a Senior Fellow at IASS on a sabbatical from Physical Research Laboratory, India. He is currently an Affiliate Scholar of RIFS. Physical Research Laboratory is supported by Department of Space, Government of India.

Data availability Data used are available at https://aeronet.gsfc.nasa.gov/, http://www.esrl.noaa.gov/psd/ and https://www.ready.noaa.gov.

Declarations

Ethics approval and consent to participate Not applicable.

Consent for publication The work has not been published anywhere previously in any form, and it is not being considered for publication elsewhere. All the authors approve the publication.

Competing interests The authors declare that they have no known competing financial interests or personal relationships that could have appeared to influence the work reported in this paper.

References

Andrews E, Ogren JA, Kinne S, Samset B (2017) Comparison of AOD, AAOD and column single scattering albedo from AERONET retrievals and in situ profiling measurements. Atmos Chem Phys 17:6041–6072. https://doi.org/10.5194/acp-17-6041-2017

Ansari K, Ramachandran S (2023) Aerosol characteristics over Indo-Gangetic plain from ground-based AERONET and MERRA-2/CAMS model simulations. Atmos Env 293:119434. https://doi.org/10.1016/j.atmosenv.2022.119434

Ansari K, Ramachandran S (2024) Optical and physical characteristics of aerosols over asia: AERONET, MERRA-2 and CAMS. Atmos Env 326:120470. https://doi.org/10.1016/j.atmosenv.2024.120470

Bond TC, Doherty SJ, Fahey DW, Forster PM, Berntsen T, DeAngelo BJ, Flanner MG, Ghan S, Kärcher B, Koch D, Kinne S, Kondo Y, Quinn PK, Sarofim MC, Schultz MG, Schulz M, Venkataraman C, Zhang H, Zhang S, Bellouin N, Guttikunda SK, Hopke PK, Jacobson MZ, Kaiser JW, Klimont Z, Lohmann U, Schwarz JP, Shindell D, Storelvmo T, Warren SG, Zender CS (2013) Bounding the role of black carbon in the climate system: a scientific assessment. J Geophys Res Atmos 118:5380–5552. https://doi.org/10.1002/jgrd.50171

Cao Y, Shao L, Jones, Oliveira MLS, Ge S, Feng X, Silva LFO, Bérub K (2021) Multiple relationships between aerosol and COVID19: A framework for global studies. Gondwana Res 93:243–251

Che Y, Yu B, Parsons K, Desha C, Ramezani M (2022) Evaluation and comparison of MERRA-2 AOD and DAOD with MODIS deepblue and AERONET data in Australia. Atmos Environ 277:119054. https://doi.org/10.1016/j.atmosenv.2022.119054

Cho C, Kim S-W, Rupakheti M, Park J-S, Panday A, Yoon S-C, Kim J-H, Kim H, Jeon H, Sung M, Kim BM, Hong SK, Park RJ, Rupakheti D, Mahata KS, Praveen PS, Lawrence MG, Holben B (2017) Wintertime aerosol optical and radiative properties in the Kathmandu Valley during the SusKat-ABC field campaign. Atmos Chem Phys 17:12617–12632. https://doi.org/10.5194/acp-17-12617-2017

Decesari S, Facchini MC, Carbone C, Giulianelli L, Rinaldi M, Finessi E, Fuzzi S, Marinoni A, Cristofanelli P, Duchi R, Bonasoni P,

Vuillermoz E, Cozic J, Jaffrezo JL, Laj P (2010) Chemical composition of PM<Subscript>10</Subscript> and PM<Subscript>1</Subscript> at the high-altitude Himalayan station Nepal Climate Observatory-Pyramid (NCO-P) (5079 m a.s.l.). Atmos Chem Phys 10(10):4583–4596. https://doi.org/10.5194/acp-10-4583-2010

Dey. S, Di Girolamo L (2011) A decade of change in aerosol properties over the Indian subcontinent. Geophys Res Lett 38:L14811. https://doi.org/10.1029/2011GL048153

Draxler RR, Hess GD (1998) An overview of the HYSPLIT-4 modelling system for trajectories, dispersion and deposition. Aust Meteorol Mag 47:295e308

Dubovik O, Smirnov A, Holben BN, King MD, Kaufman YJ, Eck TF, Schuster I (2000) Accuracy assessments of aerosol optical properties retrieved from aerosol robotic network (AERONET) sun and sky radiance measurements. J Geophys Res 105:9791–9806

Dubovik O, Holben B, Eck TF, Smirnov A, Kaufman YJ, King MD, Tanre D, Slutsker I (2002) Variability of absorption and optical properties of key aerosol types observed in worldwide locations. J Atmos Sci 59:590–608

Eck TF, Holben BN, Sinyuk A, Pinker RT, Goloub P, Chen H, Chatenet B, Li Z, Singh RP, Tripathi SN, Reid JS, Giles DM, Dubovik O, O'Neill NT, Smirnov A, Wang P, Xia X (2010) Climatological aspects of the optical properties of fine/coarse mode aerosol mixtures. J Geophys Res 115:D19205. https://doi.org/10.1029/2010JD014002

Filonchyk M, Peterson M, Yan H, Yang S, Chaikovsky A (2021) Columnar optical characteristics and radiative properties of aerosols of the AERONET site in Minsk, Belarus. Atmos Environ 249:118237. https://doi.org/10.1016/j.atmosenv.2021.118237

Forster P, Storelvmo T, Armour K, Collins W, Dufresne J-L, Frame D, Lunt DJ, Mauritsen T, Palmer MD, Watanabe M, Wild M, Zhang H (2021) The Earth's Energy Budget, Climate Feedbacks, and Climate Sensitivity. In Climate Change 2021: The Physical Science Basis. Contribution of Working Group I to the Sixth Assessment Report of the Intergovernmental Panel on Climate Change [Masson-Delmotte, V., P. Zhai, A. Pirani, S.L. Connors, C. Péan, S. Berger, N. Caud, Y. Chen, L. Goldfarb, M.I. Gomis, M. Huang, K. Leitzell, E. Lonnoy, J.B.R. Matthews, T.K. Maycock, T. Waterfield, O. Yelekçi, R. Yu, and B. Zhou (eds.)]. Cambridge University Press, Cambridge, United Kingdom and New York, NY, USA, pp. 923–1054, https://doi.org/10.1017/9781009157896.009

Gautam R, Hsu NC, Tsay SC, Lau KM, Holben B, Bell S, Smirnov A, Li C, Hansell R, Ji Q, Payra S, Aryal D, Kayastha R, Kim KM (2011) Accumulation of aerosols over the Indo-Gangetic plains and Southern slopes of the Himalayas: distribution, properties and radiative effects during the 2009 pre-monsoon season. Atmos Chem Phys 11:12841–12863. https://doi.org/10.5194/acp-11-12841-2011

Giles DM, Holben BN, Tripathi SN, Eck TF, Newconb WW, Slutsker I, Dickerson RR, Thompson AM, Mattoo S, Wang S-H, Singh RP, Sinyuk A, Schafer JJ (2011) Aerosol properties over the Indo-Gangetic Plain: a mesoscale perspective from the TIGERZ experiment. J Geophys Res 116:D18203. https://doi.org/10.1029/2011JD015809

Giles DM, Holben BN, Eck TF, Sinyuk A, Smirnov A, Slutsker I, Dickerson RR, Thompson AM, Schafer JJ (2012) An analysis of AERONET aerosol absorption properties and classifications representative of aerosol source regions. J Geophys Res 117:D17203. https://doi.org/10.1029/2012JD018127

Gueymard CA, Yang D (2020) Worldwide validation of CAMS and MERRA-2 reanalysis aerosol optical depth products using 15 years of AERONET observations. Atmos Environ 225:117216. https://doi.org/10.1016/j.atmosenv.2019.117216

Gustafsson O, Ramanathan V (2016) Convergence on climate warming by black carbon aerosols. Proc Natl Acad Sci USA 113:4243–4245

Gustafsson Ö, Krusa M, Zencak Z, Sheesley RJ, Granat L, Engström E, Praveen PS, Rao PSP, Leck C, Rodhe H (2009) Brown clouds over South Asia: biomass or fossil fuel combustion. Science 323:495–498

Hess M, Koepke P, Schult I (1998) Optical properties of aerosols and clouds: the software package OPAC. Bull Am Meteorol Soc 79:831–844

Holben BN, Tanré D, Smirnov A, Eck TF, Slutsker I, Abuhassan N, Newcomb WW, Schafer JS, Chatenet B, Lavenu F, Kaufman YJ, Castle JV, Setzer A, Markham B, Clark D, Frouin R, Halthore R, Karneli A, O'Neill NT, Pietras C, Pinker RT, Voss K, Zibordi G (2001) An emerging ground-based aerosol climatology: aerosol optical depth from AERONET. J Geophys Res 106:12067–12097

Jethva H, Chand D, Torres O, Gupta P, Lyapustin A, Patadia F (2018) Agricultural burning and air quality over northern India: a synergistic analysis using NASA's A-train satellite data and ground measurements. Aerosol Air Qual Res 18:1756–1773. https://doi.org/10.4209/aaqr.2017.12.0583

Kedia S, Ramachandran S, Tripathi SN, Holben B (2014) Quantification of aerosol type, and sources of aerosols over the Indo-Gangetic plain. Atmos Environ 98:607–619

Krishnan R, Shrestha AB, Ren G, Rajbhandari R, Saeed S, Sanjay J, Syed MA, Vellore R, Xu Y, You Q, Ren Y (2019) Unravelling climate change in the Hindu Kush Himalaya: Rapid warming in the mountains and increasing extremes in *The Hindu Kush Himalaya Assessment*, P. Wester, A. Mishra, A. Mukherji and A.B. Shrestha (eds.), 57–97 pp

Kuhlmann J, Quaas J (2010) How can aerosols affect the Asian summer monsoon? Assessment during three consecutive pre-monsoon seasons from CALIPSO satellite data. Atmos Chem Phys 10:4673–4688. https://doi.org/10.5194/acp-10-4673-2010

Lawrence MG, Lelieveld J (2010) Atmospheric pollutant outflow from Southern Asia: a review. Atmos Chem Phys 10:11017–11096. https://doi.org/10.5194/acp-10-11017-2010

Levy RC, Mattoo S, Munchak LA, Remer LA, Sayer AM, Patadia F, Hsu NC (2013) The collection 6 MODIS aerosol products over land and ocean. Atmos Meas Tech 6:2989–3034

Li W, Shao L, Wang W, Li H, Wang X, Li Y, Li W, Jones T, Zhang D (2020) Air quality improvement in response to intensified control strategies in Beijing during 2013–2019. Sci Total Environ 744:140776. https://doi.org/10.1016.j/scitotenv.2020.140776

Liu H, Yang F, Du Y, Ruan R, Tan H, Xiao J, Zhang S (2019) Field measurements on particle size distributions and emission characteristics of PM10 in a cement plant of China. Atmos Poll Res 10:1464–1472. https://doi.org/10.1016/j.apr.2019.04.003

Myhre G, Samset BH, Schulz M, Balkanski Y, Bauer S, Berntsen TK, Bian H, Bellouin N, Chin M, Diehl T, Easter RC, Feichter J, Ghan SJ, Hauglustaine D, Iversen T, Kinne S, Kirkevåg A, Lamarque J-F, Lin G, Liu X, Lund MT, Luo G, Ma X, van Noije T, Penner JE, Rasch PJ, Ruiz A, Seland Ø, Skeie RB, Stier P, Takemura T, Tsigaridis K, Wang P, Wang Z, Xu L, Yu H, Yu F, Yoon J-H, Zhang K, Zhang H, Zhou C (2013) Radiative forcing of the direct aerosol effect from AeroCom Phase II simulations. Atmos Chem Phys 13:1853–1877. https://doi.org/10.5194/acp-13-1853-2013

O'Neill NT, Eck TF, Smirnov A, Holben BN, Thulasiraman S (2003) Spectral discrimination of coarse and fine mode optical depth. J Geophys Res 108. https://doi.org/10.1029/2002JD002975

Paulot F, Naik V, Horowitz LW (2022) Reduction in near-surface wind speeds with increasing CO_2 may worsen winter air quality in the Indo-Gangetic Plain. Geophys Res Lett 49:e2022GL099039. https://doi.org/10.1029/2022gl099039

Popp et al (2016) Development, production and evaluation of aerosol climate data records from european satellite observations (Aerosol_cci). Rem Sens 8:421. https://doi.org/10.3390/rs8050421

Prasad AK, Singh RP (2007) Comparison of MISR-MODIS aerosol optical depth over the Indo-Gangetic basin during the

winter and summer seasons (2000–2005). Remote Sens Environ 107:109–119

Putero D, Marinoni A, Bonasoni P, Calzolari F, Rupakheti M, Cristofanelli P (2018) Black carbon and Ozone variability at the Kathmandu Valley and at the Southern Himalayas: a comparison between a hot spot and a downwind high-altitude site. Aero Air Qual Res 18:623–635. https://doi.org/10.4209/aaqr.2017.04.0138

Raatikainen T, Hyvärinen A-P, Hatakka J, Panwar TS, Hooda RK, Sharma VP, Lihavainen H (2014) The effect of boundary layer dynamics on aerosol properties at the Indo-Gangetic plains and at the foothills of the Himalayas. Atmos Environ 89:548–555. https://doi.org/10.1016/j.atmosenv.2014.02.058

Ramachandran S (2018) Atmospheric aerosols: Characteristics and radiative effects. CRC Press, Taylor and Francis Group, USA, p 294

Ramachandran S, Kedia S (2013) Aerosol optical properties over South Asia from ground-based observations and remote sensing: a review. Climate 1:84–119. https://doi.org/10.3390/cli1030084

Ramachandran S, Rupakheti M (2021) Inter-annual and seasonal variations in optical and physical characteristics of columnar aerosols over the Pokhara Valley in the Himalayan foothills. Atmos Res 248:105254. https://doi.org/10.1016/j.atmosres.2020.105254

Ramachandran S, Kedia S, Sheel V (2015) Spatiotemporal characteristics of aerosols in India: observations and model simulations. Atmos Env 116:225–244. https://doi.org/10.1016/j.atmosenv.2015.06.015

Ramachandran S, Rupakheti M, Lawrence MG (2020) Aerosol-induced atmospheric heating rate decreases over South and East Asia as a result of changing content and composition. Sci Rep. https://doi.org/10.1038/s41598-020-76936-z

Ramachandran S, Rupakheti M (2022) Trends in physical, optical and chemical columnar aerosol characteristics and radiative effects over South and East Asia: Satellite and ground-based observations. Gondwana Research 105:366–387. https://doi.org/10.1016/j.gr.2021.09.016

Ramachandran S, Rupakheti M, Cherian R (2022) Insights into recent aerosol trends over Asia from observations and CMIP6 simulations. Sci Total Environ 807:150756. https://doi.org/10.1016/j.scitotenv.2021.150756

Ramanathan V, Li F, Ramana MV, Praveen PS, Kim D, Corrigan CE, Nguyen H, Stone EA, Schauer JJ, Carmichael GR, Adhikary B, Yoon SC (2007) Atmospheric brown clouds: hemispherical and regional variations in long-range transport, absorption, and radiative forcing. J Geophys Res. https://doi.org/10.1029/2006JD008124

Rubin JI, Reid JS, Hansen JA, Anderson JL, Holben BN, Xian P, Westphal DL, Zhang J (2017) Assimilation of AERONET and MODIS AOT observations using variational and ensemble data assimilation methods and its impact on aerosol forecasting skill. J Geophys Res 122:4967–4992. https://doi.org/10.1002/2016JD02067

Rupakheti D, Kang S, Rupakheti M, Cong Z, Panday AK, Holben BN (2019) Identification of absorbing aerosol types at a site in the Northern edge of Indo-Gangetic plain and a polluted Valley in the foothills of the central Himalayas. Atmos Res 223:15–23. https://doi.org/10.1016/j.atmosres.2019.03.003

Rupakheti D, Rupakheti M, Abdullaev SF, Yin X, Kang S (2020) Columnar aerosol properties and radiative effects over Dushanbe, Tajikistan in Central Asia. Environ Pollut 265:114872. https://doi.org/10.1016/j.envpol.2020.114872

Samset BH, Lund MT, Bollasina M, Myhre G, Wilcox L (2019) Emerging Asian aerosol patterns. Nat Geosci 12:582–586

Schutgens N, Tsyro S, Gryspeerdt E, Goto D, Weigum N, Schulz M, Stier P (2017) On the spatio-temporal representativeness of observations. Atmos Chem Phys 17:9761–9780. https://doi.org/10.5194/acp-17-9761-2017

Singh RP, Dey S, Tripathi SN, Tare V (2004) Variability of aerosol parameters over Kanpur, northern India. J. Geophys, Res. 109:D23206. https://doi.org/10.1029/2004JD004966

Singh A, Mahata KS, Rupakheti M, Junkermann W, Panday AK, Lawrence MG (2019) An overview of airborne measurement in Nepal – part 1: vertical profile of aerosol size, number, spectral absorption, and meteorology. Atmos Chem Phys 19:245–258. https://doi.org/10.5194/acp-19-245-2019

Sinyuk A, Holben BN, Eck TF, Giles DM, Slutsker I, Korkin S, Schafer JS, Smirnov A, Sorokin M, Lyapustin A (2020) The AERONET version 3 aerosol retrieval algorithm, associated uncertainties and comparisons to version 2. Atmos Meas Tech 13:3375–3411. https://doi.org/10.5194/amt-13-3375-2020

Textor C, Schulz M, Guibert S, Kinne S, Balkanski Y, Bauer S, Berntsen T, Berglen T, Boucher O, Chin M, Dentener F, Diehl T, Easter R, Feichter H, Fillmore D, Ghan S, Ginoux P, Gong S, Grini A, Hendricks J, Horowitz L, Huang P, Isaksen I, Iversen I, Kloster S, Koch D, Kirkevåg A, Kristjansson JE, Krol M, Lauer A, Lamarque JF, Liu X, Montanaro V, Myhre G, Penner J, Pitari G, Reddy S, Seland Ø, Stier P, Takemura T, Tie X (2006) Analysis and quantification of the diversities of aerosol life cycles within AeroCom. Atmos Chem Phys 6:1777–1813. https://doi.org/10.5194/acp-6-1777-2006

Tripathee L, Kang S, Rupakheti D, Cong Z, Zhang Q, Huang J (2017) Chemical characteristics of soluble aerosols over the central Himalayas: insight into spatiotemporal variations and sources. Environ Sci Pollut Res Int 24:24454–24472. https://doi.org/10.1007/s11356-017-0077-0

World Air Quality Report (2020) https://www.iqair.com. 41 pp

Zhang Q, Zheng Y, Tong D, Shao M, Wang S, Zhang Y, Xu X, Wang J, He H, Liu W, Ding Y, Lei Y, Li J, Wang Z, Zhang X, Wang Y, Cheng J, Liu Y, Shi Q, Yan L, Geng G, Hong C, Li M, Liu F, Zheng B, Cao J, Ding A, Gao J, Fu Q, Huo J, Liu B, Liu Z, Yang F, He K, Hao J (2019) Drivers of improved $PM_{2.5}$ air quality in China from 2013 to 2017. Proc Natl Acad Sci USA 116:24463–24469. https://doi.org/10.1073/pnas.1907956116

Zhou M, Xie Y, Wang C, Shen L, Mauzerall DL (2024) Impacts of current and climate induced changes in atmospheric stagnation on Indian surface PM2.5 pollution. Nat Commun. https://doi.org/10.1038/s41467-024-51462-y